

Vapor-Dominated Zones Within Hydrothermal Systems: Evolution and Natural State

S. E. INGEBRITSEN AND M. L. SOREY

U.S. Geological Survey, Menlo Park, California

Three conceptual models illustrate the range of hydrothermal systems in which vapor-dominated conditions are found. The first model (model I) represents a system with an extensive near-vaporstatic vapor-dominated zone and limited liquid throughflow and is analogous to systems such as The Geysers, California. Such systems can evolve within low-permeability barriers without changes in boundary conditions or rock properties, given an adequate supply of heat. Their scarcity in nature may be due to the need for a long-lived, potent heat source and for a low-permeability aureole that remains intact for significant lengths of time. Models II and III represent systems with significant liquid throughflow and include steam-heated discharge features at higher elevations and high-chloride springs at lower elevations, connected to and fed by a single circulation system at depth. In model II, as in model I, the vapor-dominated zone has a near-vaporstatic vertical pressure gradient and is generally underpressured with respect to local hydrostatic pressure. The vapor-dominated zone in model III is quite different, in that phase separation takes place at pressures close to local hydrostatic and the overall pressure gradient is near hydrostatic. A relatively large number of high-temperature systems in regions of moderate to great topographic relief are similar to either model II or model III; however, in most cases there are insufficient data to establish a single preferred model.

INTRODUCTION

Naturally occurring hydrothermal systems can be broadly categorized as either vapor-dominated or liquid-dominated. Within part of a vapor-dominated system, steam is the pressure-controlling phase. Vapor-dominated conditions within natural hydrothermal systems may be extensive areally (to tens of square kilometers) and vertically (to more than 3 km depth), as at The Geysers, California, or they may be very localized, confined to a few fractures or fracture zones. Although the model of vapor-dominated hydrothermal systems formulated by *White et al.* [1971] is generally accepted, how vapor-dominated systems evolve and how they behave in the natural state is not well-understood, partly because of their scarcity and partly because of the difficulty of quantitatively describing two-phase systems.

This paper presents simulations of model systems that represent a range of hydrothermal systems within which vapor-dominated conditions are found. We investigate the conditions that allow each system to evolve and relate the simulated behavior of the model systems to the observed characteristics of certain natural systems.

The conceptual models used as a basis for numerical simulation range from a system with an extensive vapor-dominated zone that is generally underpressured with respect to the local hydrostatic pressure (Figure 1a, model I) to a system that includes a very localized vapor-dominated zone at pressures above local hydrostatic (Figure 1c, model III). Model I-like systems lack significant liquid throughflow, while the vapor-dominated zones in models II and III are both "parasitic" to underlying flows of boiling water that also feed thermal springs at lower elevations. Although each model has unique features, they have some characteristics in common. They each involve phase separation at pressures significantly greater than atmospheric and include zones in which vapor is by far the more mobile phase (relative to liquid water). Fumaroles and

steam-heated acid-sulfate springs would be associated with systems similar to each model, as a result of the phase separation and surficial discharge of steam.

Most natural systems are significantly more complex than the models shown in Figure 1, and many would be better represented as a combination of the models. Systems such as The Geysers (California, United States), Larderello (Italy), Kamojang (Indonesia), and Matsukawa (Japan) are generally similar to model I. A relatively large number of high-temperature systems in regions of moderate to great topographic relief are similar to either model II or model III; however, in most cases the thickness and pressure distribution within the vapor-dominated zone are unknown.

Any distinction between vapor- and liquid-dominated conditions based on the vertical pressure gradient, the relative mass flux of steam and liquid q_s/q_w , or relative permeabilities k_{rs}/k_{rw} is somewhat arbitrary. This can be deduced from Figure 2, where q_s/q_w is plotted against the logarithm of k_{rs}/k_{rw} .

Near-vaporstatic vapor-dominated zones (as in models I and II) would presumably fall within the lightly patterned region of Figure 2. Within this region there is vapor-liquid counterflow, with the vapor flux greater than the liquid flux, and the pressure gradient is less than 25% of hydrostatic. Vapor-dominated zones like the one in model III might fall to the left of the lightly patterned region or below the horizontal midline of the diagram (with $|q_s/q_w| > 1$ and $k_{rs}/k_{rw} \gg 1$). For the purposes of this study, vapor-dominated zones are considered to be those with $|q_s/q_w| > 1$ and $k_{rs}/k_{rw} \gg 1$. A criterion based only on the vertical pressure gradient would not include model III, where the pressure gradient within the vapor-dominated zone may be high despite very low liquid mobility. We will generally refer to vapor-dominated zones rather than vapor-dominated systems, because in models II and III vapor-dominated conditions encompass only a small percentage of the total flow system.

White et al. [1971] proposed a conceptual model of vapor-dominated hydrothermal systems and compared such systems to the more common liquid-dominated or hot water type.

This paper is not subject to U.S. copyright. Published in 1988 by the American Geophysical Union.

Paper number 88JB03257.

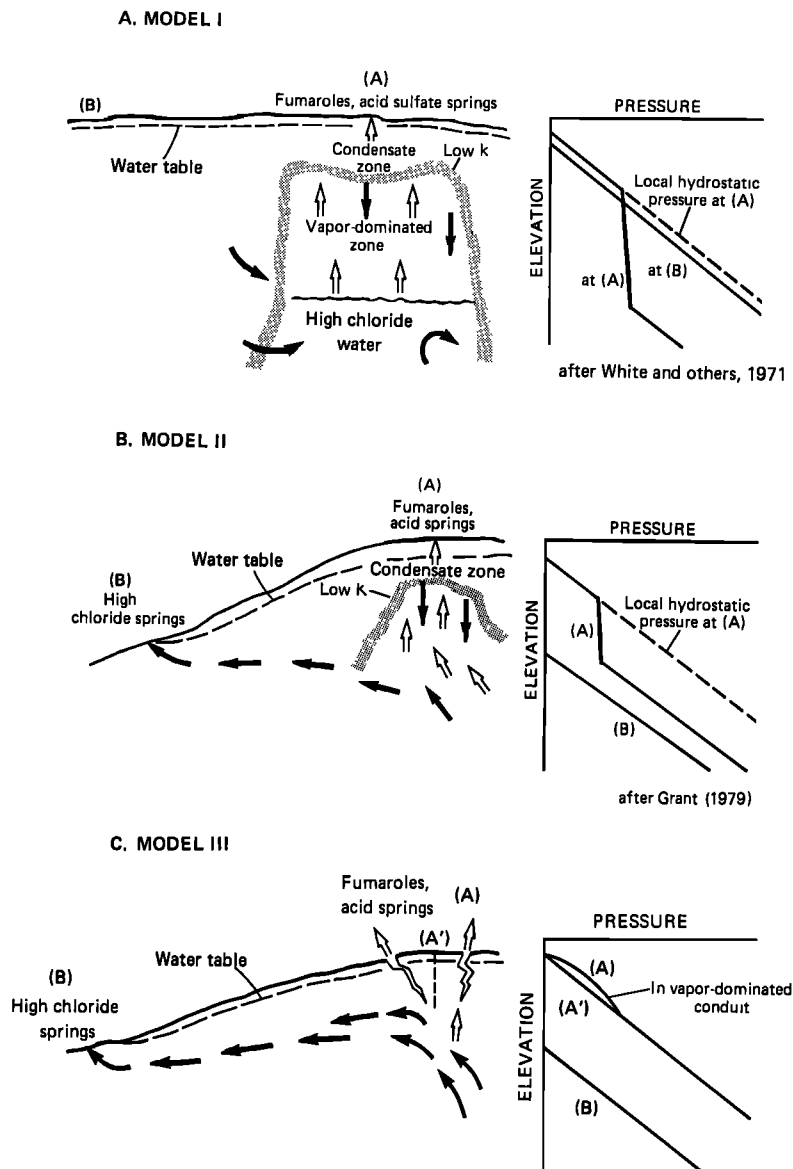


Fig. 1. Conceptual models of three hydrothermal convection systems that include vapor-dominated zones. Solid arrows are for liquid, and open arrows are for steam. (a) Representation of model I; the vapor-dominated zone is large and there is limited liquid throughflow. (b) Representation of model II. (c) Representation of model III. Models II and III both involve lateral flow that links acid-sulfate features at higher elevations with high-chloride discharge at lower elevations.

Interpreted broadly, the White et al. model incorporates all three of the models shown in Figure 1, though it was based primarily on observations at The Geysers and Larderello (systems similar to model I). The essence of this model is that within part of a vapor-dominated system steam is the pressure-controlling phase and that springs fed by vapor-dominated systems are low in chloride, gassy, and generally acidic. In contrast, waters from liquid-dominated systems are generally high in chloride and silica and have a near-neutral pH.

The difference in chemistry between the acid-sulfate waters associated with vapor-dominated conditions and the high-chloride waters from liquid-dominated systems is attributable to the relative volatility of common constituents of thermal waters, i.e., chloride and silica have low volatility in low-pressure steam, while CO_2 , H_2S , and other volatile constituents evolve along with steam. We will consistently refer to

waters from which steam has separated as "high-chloride" waters to distinguish them from the low-chloride steam and steam condensate. Particularly in models II and III the chloride concentration is not necessarily high in absolute terms. In model I there is potential for a concentrated brine to evolve below the vapor-dominated zone, as discussed by White et al. [1971], but simple mass balance calculations show that this would not happen over the time periods that we simulate.

PREVIOUS WORK

There has been limited quantitative analysis of the physical processes controlling the evolution and natural state of vapor-dominated zones. This is largely attributable to the lack of analytical solutions to geologically meaningful two-phase flow problems and to the computational difficulty and expense of simulating two-phase flow problems numerically over time scales of geologic interest.

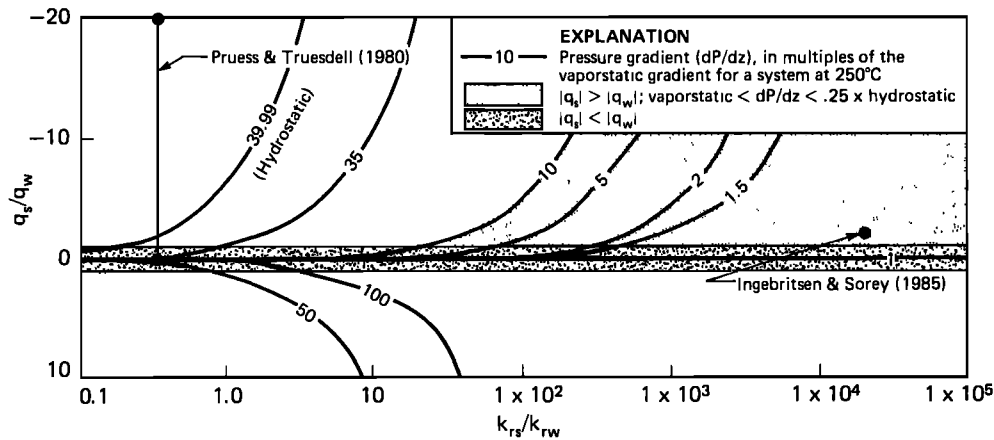


Fig. 2. Relationship between the vertical mass flux ratio of steam to liquid (q_s/q_w) and the relative permeability ratio (k_{rs}/k_{rw}) for various vertical pressure gradients. A pressure gradient of one is vaporstatic. Negative values on the ordinate indicate regions of counterflow. At any vertical pressure gradient and at a fixed pressure and temperature (so that density and viscosity are constant) q_s/q_w is linearly related to k_{rs}/k_{rw} by Darcy's Law. A semilog plot is used here to allow a wide range of values of k_{rs}/k_{rw} to be displayed.

Schubert and Straus [1979, 1980] and Straus and Schubert [1981] modeled certain aspects of vapor-dominated zones analytically. Their use of analytical methods generally restricted them to steady state one-dimensional problems involving homogeneous rock properties and constant fluid properties, and in some cases required additional simplifying assumptions. Relevant results from this work are discussed in greater detail below.

Pruess and Truesdell [1980] attempted to simulate the evolution of a vapor-dominated zone numerically with a radial fluid flow model involving conductive heat flow at the lower boundary (approximately 1.25 W m^{-2}), a constant pressure-temperature condition at the upper boundary, and no-flow lateral boundaries. Their steady state result involved a zone of two-phase counterflow below a 400-m-thick low-permeability ($3 \times 10^{-16} \text{ m}^2$) caprock. Within this two-phase zone k_{rs}/k_{rw} was approximately 0.3, so the pressure gradient was necessarily near hydrostatic, assuming that q_s/q_w was near unity (see Figure 2). A slightly higher rate of heat input might have led to a near-vaporstatic vapor-dominated zone below the caprock (see Figure 11 below).

Ingebritsen and Sorey [1985], Sorey and Ingebritsen [1984], and Ingebritsen [1983] simulated the evolution and natural state of a "parasitic" vapor-dominated zone overlying and fed by a lateral flow of thermal water. The pressure gradient in the vapor-dominated zones in their simulations was near-vaporstatic (see Figure 2). Relevant results from this work are summarized below in the context of model II.

Most recently, Pruess [1985] demonstrated numerically that a brief period of limited discharge through a low-permeability caprock could cause a transition from "liquid-dominated heat pipe" conditions (a slightly subhydrostatic pressure gradient with boiling-point-with-depth temperature distribution) to vapor-dominated conditions. With the exception of the controlled discharge event, the system was treated as closed.

Governing Equations and Numerical Methods

The conceptual models shown in Figure 1 were simulated using a modified version of the GEOTHER code [Faust and Mercer, 1979a, b; 1982; Mercer and Faust, 1979], which uses

finite difference techniques to simulate transient three-dimensional single- and two-phase heat and mass transport in a porous medium. The nonlinear governing equations are posed in terms of pressure and enthalpy and are discussed in the appendix. Modifications to the original GEOTHER code and the limitations of the code with respect to the natural systems modeled are discussed by Ingebritsen [1986].

Important assumptions inherent in the mathematical model are that Darcy's Law is valid, that there is thermal equilibrium between phases, and that capillary pressure effects are negligible. Temperatures, saturation, and fluid densities are calculated as functions of pressure and enthalpy, fluid viscosities are calculated as functions of temperature, and relative permeabilities are treated as nonhysteretic functions of volumetric saturation. Rock enthalpy is treated as a linear function of temperature and porosity is linearly related to pressure by rock compressibility. Porosities, permeabilities, and thermal conductivity can vary in space. For further discussion of the assumptions and constitutive relationships see Faust and Mercer [1979a] and Ingebritsen [1986].

MODEL I

Within the extensive vapor-dominated zone in model I (Figure 1a) [White et al., 1971], the vertical pressure gradient is somewhat above vaporstatic and there is steam-liquid counterflow. Vertical heat transport through the vapor-dominated zone is largely by a "heat pipe" mechanism that allows large net transport of heat with little net transport of mass, as much of the heat carried by the rising steam is released by condensation at the top of the vapor-dominated zone. The vapor-dominated zone is generally underpressured with respect to local hydrostatic pressures (Figure 1a), so, to exist, it must be isolated from surrounding nonthermal flow systems by low-permeability barriers.

The vapor-dominated zone is overlain by a "condensate" zone that is liquid saturated, or nearly so (Figure 1a). In systems like model I, the vapor-dominated zone is presumably underlain by a zone of high-temperature liquid, but there is no evidence for voluminous liquid throughflow.

The acidity of the associated springs (Figure 1a) is due to near-surface oxidation of H_2S that evolves along with steam

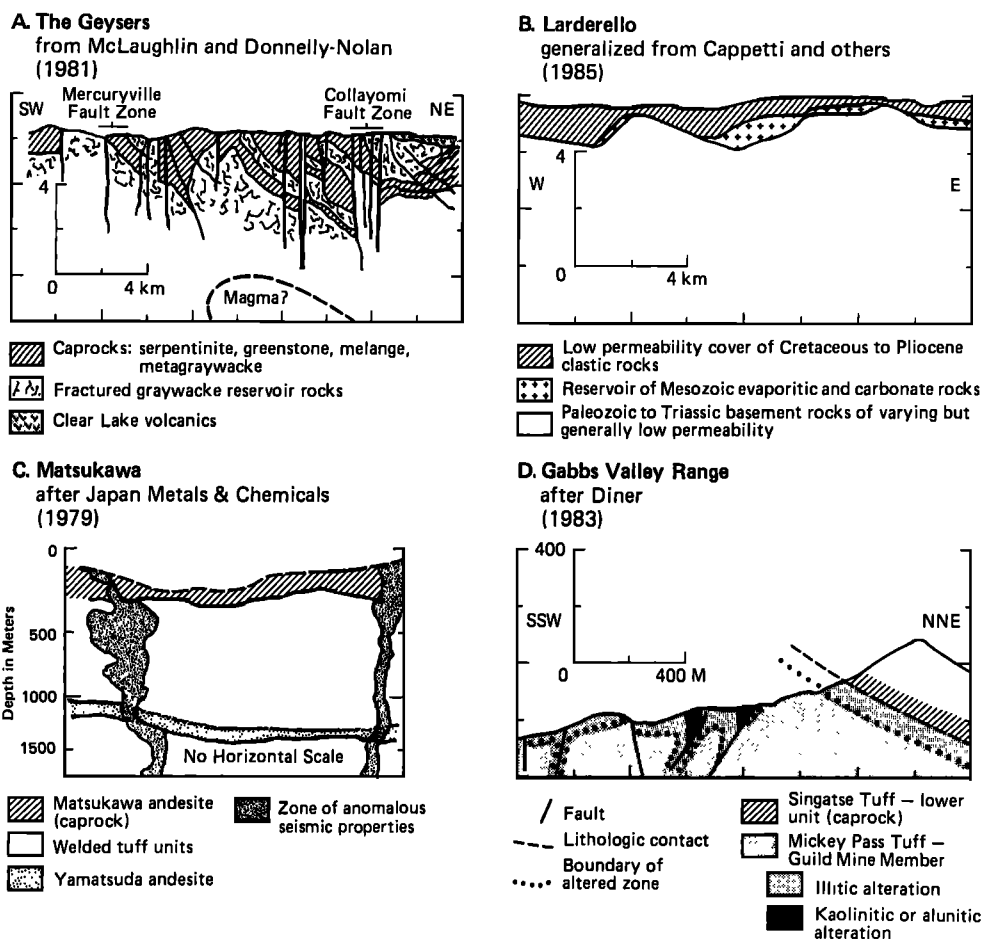


Fig. 3. Simplified geologic cross sections of natural systems that are similar to model I showing the low-permeability barriers that bound the vapor-dominated zones. At The Geysers, argillic alteration apparently helps to seal the top of the vapor-dominated zone [Hebein, 1985], which may be bounded laterally, at least in part, by mineralization along the Mercuryville and Collayomi fault zones (D. E. White, written communication, 1986). At Larderello, low-permeability shales and sandstones isolate vapor-dominated zones in carbonate rocks both vertically and laterally. At Matsukawa, the vapor-dominated zone appears to be bounded laterally by faults, though there is no evidence for mineralization along the fault zones (K. Sato, oral communication, 1986). At a possible fossil vapor-dominated system in the Gabbs Valley Range, Nevada, the pattern of mineralization below the caprock suggests that several fault zones may have comprised laterally isolated vapor-dominated heat pipes.

at the base of the vapor-dominated zone. The ground surrounding the springs is commonly bleached and altered, containing clay and sulfate minerals and native sulfur. The presence of such acid-sulfate springs, and, more directly, the presence of fumaroles, is evidence for vapor-dominated conduits through the condensate zone.

The active hydrothermal systems at The Geysers, Larderello, Kamojang, and Matsukawa are crudely similar to model I. Wells completed in the vapor-dominated zones at these systems produce saturated or (at later stages) superheated steam and little or no liquid water. Pressures in the upper parts of the vapor-dominated zones at The Geysers, Larderello, and Kamojang are generally near 30–35 bars, and the vertical pressure gradients within the vapor-dominated zones are near vaporstatic.

The low-permeability aureole surrounding the vapor-dominated zone (Figure 1a) may be related to deposition of silica, calcite, or gypsum, as discussed by White *et al.* [1971], to argillization, to geologic structure and lithologic contrasts, or to a combination of these factors. Several examples are shown in Figure 3.

Isolation due to self-sealing, by deposition of silica due to cooling in relatively shallow parts of a system, or by deposition of calcite, gypsum, or anhydrite as recharge water warms at depth, is likely to be effective during a liquid-dominated stage that precedes development of vapor-dominated conditions, as well as at later stages when recharge water enters, is heated, and vaporizes. At Reykjanes, Iceland, self-sealing by silica and calcite sustains a pressure difference of nine bars across the lateral boundaries of a high-temperature, liquid-dominated zone at a depth of 1600 m [Tomasson and Smarason, 1985]. There is mineralogic evidence for an early high-temperature liquid-dominated stage at both The Geysers [e.g., Hebein, 1985] and Matsukawa [Sumi, 1968]. Hydrothermal mineralization tends to increase preexisting permeability contrasts; for example, it tends to be more intense below low-permeability “capping” layers (for example, Figure 3d).

Geometric Model

The geometric models shown in Figure 4 were used to represent model I (Figure 1a) and, in a generalized fashion, the natural systems shown in Figure 3. Heat and mass transport

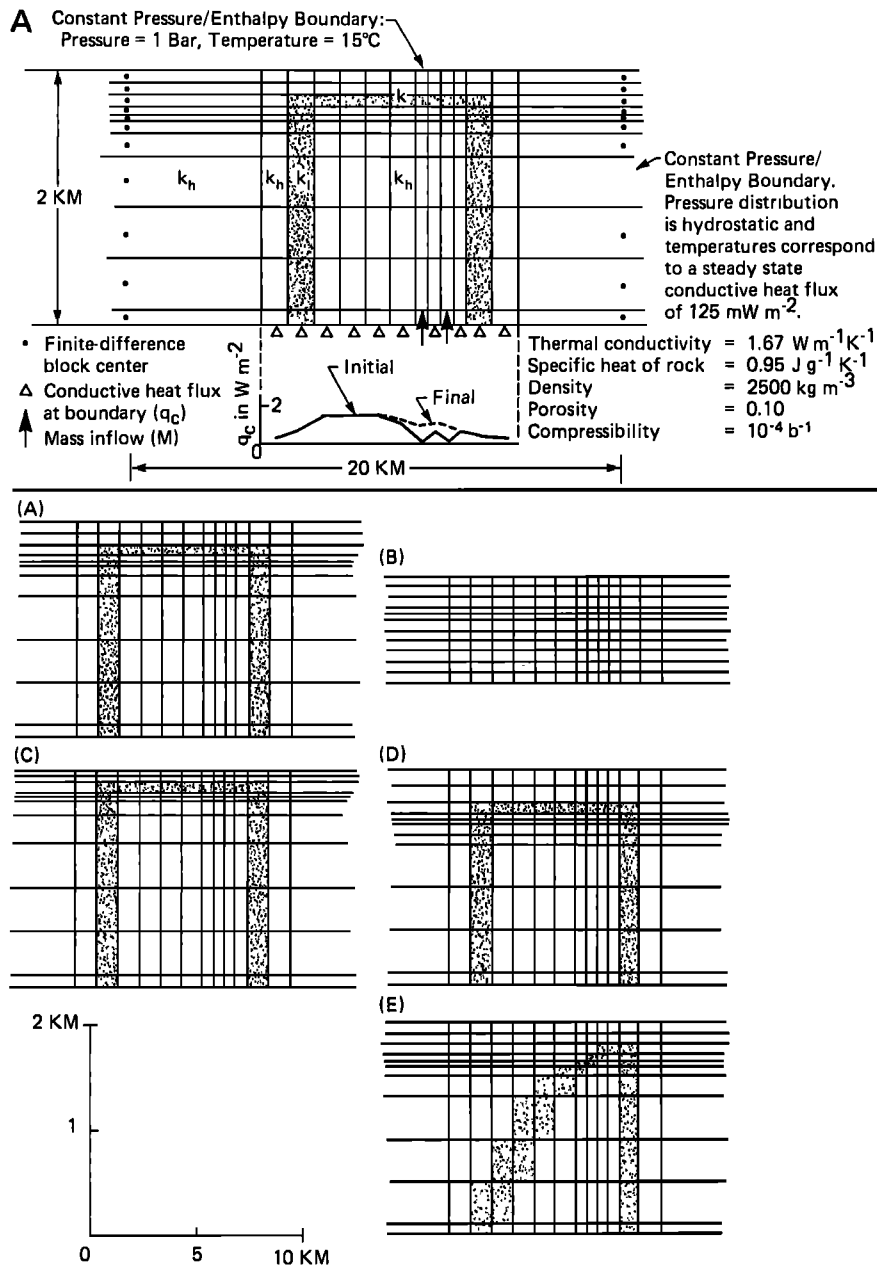


Fig. 4. Geometric models used in numerical simulations of model I. The vertical sections are 1 km thick. Values of k_h and k_1 used in various simulations are listed in Table 1 below.

within these geometric models was simulated using the computer code described above and in the appendix. The geometric models are two-dimensional vertical cross sections, with all boundaries open to mass and energy. The land surface is treated as a uniform constant pressure-enthalpy boundary at a pressure of 1 bar and an enthalpy equivalent to 15°C. The constant pressure-enthalpy lateral boundaries represent normally pressured, nonthermal flow systems. The interior of the system is isolated from these boundaries to some extent by low-permeability barriers (k_1). The lower boundary is a controlled flux boundary. Some of the numerical simulations of model I involve only conductive heat flux q_c at this boundary, and some involve mass inflow M as well as conduction.

These geometric models represent the vapor-dominated zone as an open system. Previous quantitative analyses of such large-scale vapor-dominated zones have involved models

with closed boundaries [Pruess and Truesdell, 1980; Pruess et al., 1983; Pruess, 1985] and/or dealt with less global representations of the system [Schubert and Straus, 1979, 1980; Straus and Schubert, 1981; Pruess, 1985].

In our simulations we assumed that the permeability structure (Figure 4: k_h and k_1) predates the hydrothermal system, that is, permeability is held constant. For some of the natural systems shown as examples in Figure 3 this is quite appropriate. In other cases the low-permeability barriers surrounding the vapor-dominated zone are largely related to hydrothermal mineralization. Since the governing equations are nonlinear, it is theoretically possible that allowing the permeability structure to evolve with time could lead to a different steady state. However, based on experimentation with various initial conditions we believe that the origin of the permeability structure does not affect the near-steady state results discussed below. It

may certainly affect the rate of evolution to near-steady state conditions.

The series of numerical experiments carried out for model I involved variations in the lower boundary condition, the geometry of the low-permeability aureole, and the permeabilities k_h and k_l . Parameter values, simulation times, and results in terms of the development of an extensive vapor-dominated zone are listed in Table 1.

Initial Conditions and Final States

Initial conditions for all of the simulations were a hydrostatic pressure distribution and a low-temperature conductive temperature regime (the same conditions that were maintained at the lateral boundaries throughout the simulations). Total simulation times ranged from 10,000 to 40,000 years. Some simulations involved a high initial mass inflow rate (Table 1, M_i) that was decreased linearly to a final rate M_f between simulation times of 3000–3500 or 5000–5500 years. These simulations tended to approach steady state in about 10,000 years and will be referred to as “decreasing recharge” cases. Other simulations involving only heat conduction q_c at the lower boundary were slower to approach steady state and will be referred to as “conductive heating” cases.

Our discussion of results for model I will focus on near-steady state conditions. It is unlikely that similar natural systems are truly steady state, because rock properties and boundary conditions are variable over periods of thousands of years, and temperatures approach steady state values very slowly in zones of low-velocity fluid circulation. However, comparison of near-steady state results is the most straightforward basis for evaluating the effects of different boundary conditions, geometries, and rock properties.

Results

The simulations indicated with parentheses in Table 1 led to extensive vapor-dominated zones with near-vaporstatic pressure gradients, while the others led only to short-lived (run 3) or very localized (runs 5 and 6) vapor-dominated conditions, or did not lead to the formation of vapor-dominated zones at all.

The simulations demonstrate the feasibility of two evolutionary pathways for model I that were originally suggested by White *et al.* [1971]: a decrease in mass inflow over time (e.g., Table 1, Run 1) and conductive heating at a constant rate with no changes in boundary conditions (e.g., run 4). Both of these processes can lead to extensive vapor-dominated zones, although the system evolves more rapidly in the decreasing recharge cases because of the rapid convective heating at early times. Figure 5 shows pressure profiles at later times during a decreasing recharge case (run 1) and a conductive heating case (run 4). Pressures are somewhat greater than hydrostatic above the vapor-dominated zone, and the vertical pressure gradient is near-vaporstatic within the vapor-dominated zone and near-hydrostatic below the vapor-dominated zone.

Pressure profiles. The excess pressure at the top of the vapor-dominated zone (Figure 5) is necessary to allow flow into the low-permeability caprock k_1 . If there is more heat coming in at the base of the system than can be transferred conductively out of the top of the vapor-dominated zone, there must be additional heat transfer by steam moving across the low-permeability caprock. This is the case in both of the examples shown in Figure 5.

In nature flow patterns are more complex than in our

simple model, probably involving vapor-dominated conduits through an otherwise liquid-saturated condensate zone. However, the same general considerations apply. Superhydrostatic pressures in shallow steam zones have been observed at The Geysers (up to approximately 150% of hydrostatic at 150 m depth) [Allen and Day, 1927], Matsukawa (M. Hanano, unpublished data, 1986), Mud Volcanoes, Yellowstone (approximately 125% of hydrostatic at 106 m depth) [White *et al.*, 1971], and Svartsengi, Iceland, where a “steam cap” is forming in response to exploitation [Gudmundsson and Thorhallsson, 1986].

The stability of the “liquid over steam” configuration at the top of the vapor-dominated zone has been considered something of an enigma, though Schubert and Straus [1980] showed that this configuration will be stable in a medium with a uniform low permeability ($< 4 \times 10^{-17} \text{ m}^2$). It will also be stable if pressures at the top of the vapor-dominated zone are somewhat above local hydrostatic, or if the pressure gradient into the base of the caprock is superhydrostatic, as in the examples discussed here.

The vapor-dominated zones in Figure 5 are only 100–200 m thick, much thinner than at The Geysers, for example. At 40,000 years the conductive heating run (run 4) is far from steady state, but the decreasing recharge run (run 1) is approaching steady state at 10,000 years. Mass and energy balances for the latter example (Figure 6) show very small rates of change in storage. Assuming that the change in mass storage in the “reservoir” bounded by the low-permeability barriers is due to replacement of liquid water by low-density steam, the thickness of the vapor-dominated zone is increasing by $< 0.03 \text{ m/year}$.

Several factors affect the equilibrium thickness of the vapor-dominated zone. The lateral pressure gradient into the vapor-dominated zone increases with the thickness of the vapor-dominated zone (Figure 5b). Eventually, the amount of lateral inflow (plus any mass inflow at the base of the system) balances the amount of steam flowing out of the vapor-dominated zone (Figure 6). Critical factors influencing the equilibrium thickness include the permeability of the barriers that inhibit lateral inflow ($k_l(1)$ in Figure 7a) and the heat input at the base of the system. An increase in the heat input would increase the rate of steam loss and require a thicker vapor-dominated zone to induce additional lateral inflow. If the lateral barriers ($k_l(1)$) were completely impermeable (preventing inflow), the vapor-dominated zone would tend to keep growing indefinitely. Of course, when the vapor-dominated zone reaches the lower boundary of the geometric model the controlled-flux condition used at this boundary is no longer appropriate.

Figure 7b shows pressure profiles at a time of 10,000 years for the decreasing recharge case shown in Figure 5 (run 1) and for a similar run (run 1A) in which $k_l(1)$ was decreased by two orders of magnitude at a time of 8500 years. The thickness of the vapor-dominated zone in the latter simulation was near equilibrium prior to the change in $k_l(1)$, but increased rapidly afterward. At 10,000 years the base of the vapor-dominated zone is approaching the lower boundary of the geometric model.

Heat input. A series of simulations (Table 1, runs 4, 1, 5, and 6) illustrates the effect of varying the final mass inflow rate M_f . Low rates of mass inflow (runs 4 and 1) lead to extensive vapor-dominated zones. Because of the low-permeability aureole moderate inflow rates lead to higher pressures such that

TABLE 1. Summary of Numerical Simulations of Model I

Run	Geometry*	$k_h, * m^2$	$k_1, * m^2$	$\bar{q}_c, \dagger W m^{-2}$	$M_i, \ddagger kg s^{-1}$	$M_f, \S kg s^{-1}$	Time to M_f , years	Total Simulation Time, years
(1)	A	1.0×10^{-13}	5.0×10^{-17}	1.09	100	2	3,500	10,000
(2)	A	1.0×10^{-13}	5.0×10^{-17}	1.09	100	2	5,500	10,000
3	A	1.0×10^{-13}	5.0×10^{-17}	0	100	2	3,500	10,000
(4)	A	1.0×10^{-13}	5.0×10^{-17}	1.09	0	0	N.A.	40,000
5	A	1.0×10^{-13}	5.0×10^{-17}	1.09	100	5	3,500	10,000
6	A	1.0×10^{-13}	5.0×10^{-17}	1.09	100	10	3,500	10,000
(7)	A	1.0×10^{-13}	5.0×10^{-19}	1.09	0	0	N.A.	40,000
8	A	1.0×10^{-13}	5.0×10^{-15}	1.09	100	2	5,500	10,000
9	B	1.0×10^{-16}	1.0×10^{-16}	1.09	0	0	N.A.	25,000
10	B	1.0×10^{-15}	1.0×10^{-15}	1.09	0	0	N.A.	25,000
(11)	C	1.0×10^{-13}	5.0×10^{-17}	1.09	100	2	3,500	10,000
(12)	D	1.0×10^{-13}	5.0×10^{-17}	1.09	100	2	3,500	10,000
(13)	E	1.0×10^{-13}	5.0×10^{-17}	1.09	100	2	3,500	10,000

Runs in parentheses led to extensive vapor-dominated zones. The Corey relative permeability functions shown in Figure 19 below were used in all of these simulations.

*See Figure 4.

†Final mean conductive heat flow at base of model. Between the low-permeability barriers the mean value is $1.53 W m^{-2}$. See Figure 4 for the distribution of q_c .

‡Initial mass inflow rate.

§Final mass inflow rate.

pressures are above hydrostatic throughout the system (runs 5 and 6). The limitation on mass inflow implies that the conductive heat input must greatly exceed the convective heat input at the lower boundary in order for an extensive vapor-dominated zone to form (Figure 8).

The high conductive heat input needed to generate a vapor-dominated zone implies an underlying heat source of great

intensity. Assuming a steady state thermal regime and no convection below the lower boundary of our model (2 km), the depth (in kilometers) to magmatic temperatures implied by the lower boundary condition is

$$D = 2 + (K_m(T_m - T_b)/\bar{q}_c) \times 10^{-3} \quad (1)$$

where K_m is thermal conductivity (assumed constant with depth and time), T_m is the magmatic temperature, T_b is the temperature at the lower boundary, and \bar{q}_c is the average conductive heat flux at the lower boundary. The average heat input in the center of the model is $1.5 W m^{-2}$, and the temperature at the base of the model equilibrates at about $300^\circ C$ in all of the simulations. For a magmatic temperature of $850^\circ C$ and a thermal conductivity value of $1.67 W m^{-1} K^{-1}$, $D = 2.6$ km. With active convection at depths below 2 km, the depth to magmatic temperatures in a steady state thermal regime could be much greater than that calculated from (1).

Permeability structure. The set of numerical experiments listed in Table 1 can be used to estimate the values of k_h and k_1 (Figure 4) required for a vapor-dominated zone to evolve. However, there are some caveats: the required permeability values are somewhat dependent on the geometry and particularly the thickness of the low-permeability aureole and it might be appropriate to consider the permeabilities of the lateral barriers ($k_1(1)$) and the caprock ($k_1(2)$) (Figure 7a) separately, as in general $k_1(2)$ affects steam flux out of the vapor-dominated zone and $k_1(1)$ affects lateral inflow. One statement that can be made a priori is that k_1 cannot be zero. Since the starting point is a liquid saturated medium, there must be some permeability to allow mass to move out of the enclosed reservoir. For $k_1 \lesssim 10^{-16} m^2$, the reservoir is sufficiently isolated from the constant pressure-enthalpy boundaries for vapor-dominated conditions to evolve. This limiting value applies to the generalized scale of the geometric model and does not rule out localized high permeability in the caprock; in fact, higher-permeability conduits must exist in nature to allow fumarolic discharge. Because of the uniformly low value of k_1 applied in the model, all of the steam rising out of the

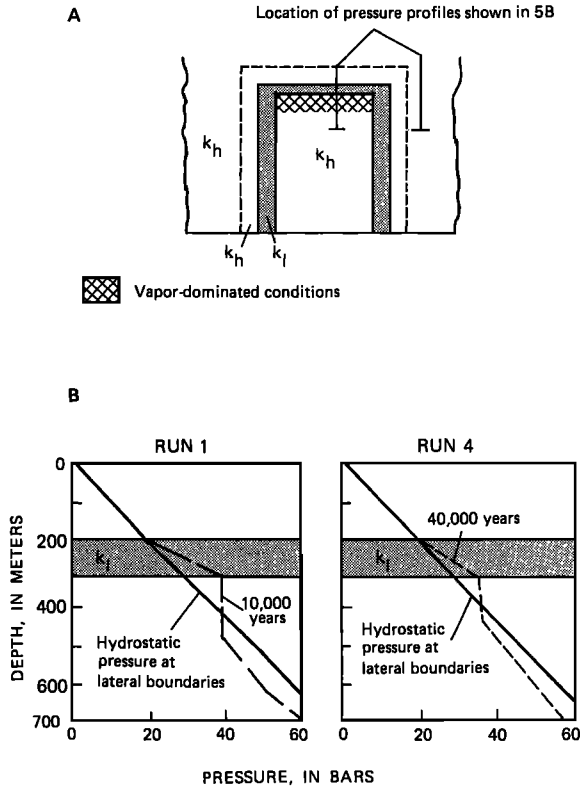
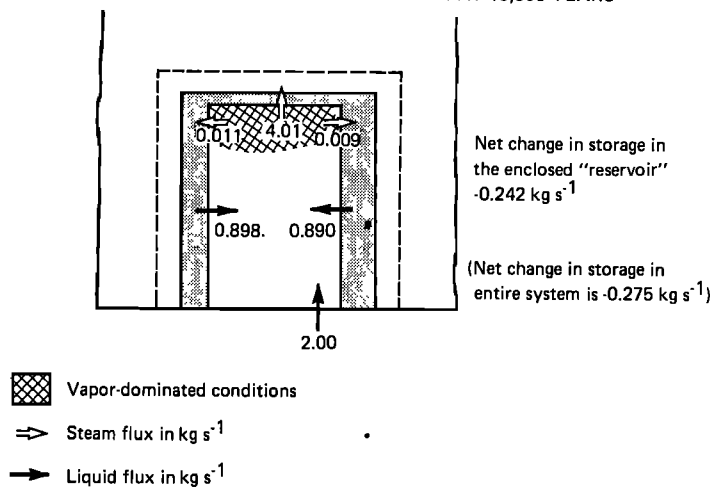


Fig. 5. (a) Location of the pressure profiles shown in Figure 5b. (b) Pressure profiles at selected times during runs 1 (a decreasing recharge case) and 4 (a conductive heating case).

MASS BALANCE FOR VAPOR-DOMINATED ZONE---RUN 1 AT 10,000 YEARS



ENERGY BALANCE FOR VAPOR-DOMINATED ZONE---RUN 1 AT 10,000 YEARS

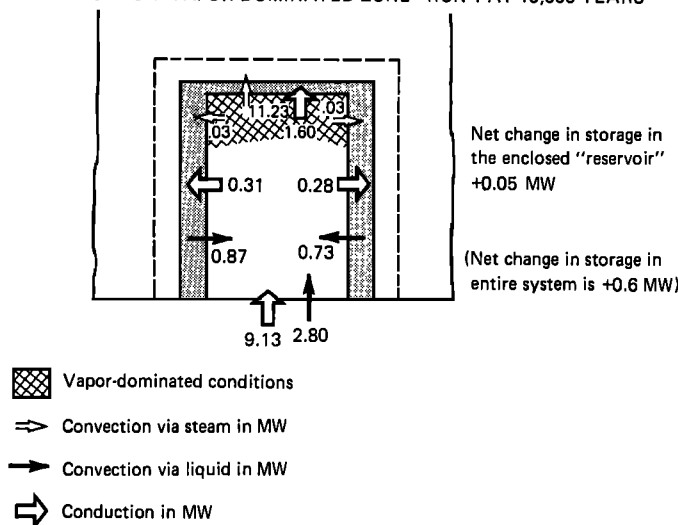


Fig. 6. Mass and energy balances for the vapor-dominated zone in run 1 (a decreasing recharge case) at a time of 10,000 years. The small rates of change in storage show that thickness of the vapor-dominated zone is increasing very slowly.

vapor-dominated zone condenses before passing out of the caprock layer. For a low reservoir permeability ($k_h \lesssim 10^{-15} \text{ m}^2$) vertical conductive heat transport is of the same magnitude or greater than convective heat transport, and no vapor-dominated zone evolved (the near-isothermal conditions within the vapor-dominated zone imply convective heat flux \gg conductive).

This set of experiments thus corroborates *Straus and Schubert's* [1981] conclusion that a permeability contrast ($k_h > k_l$) is needed to allow a vapor-dominated zone to evolve (Figure 9). Their earlier work [Schubert and Straus, 1980] had shown that a uniform permeability of $\leq 4 \times 10^{-17} \text{ m}^2$ was required for gravitational stability of water over steam. In the later work [Straus and Schubert, 1981] they found that higher permeabilities were needed within the vapor-dominated zone itself, and recognized the need for a permeability contrast at the top of the vapor-dominated zone.

Pressure in the vapor-dominated zone. The depth to the top of the vapor-dominated zone is fixed by the depth to and

thickness of the caprock; vapor-dominated zones develop immediately below such low-permeability layers and grow downwards. Near-steady state pressures within the vapor-dominated zones in these simulations varied regularly with changes in the depth from the upper pressure boundary to the low-permeability caprock (Figure 10). This is predictable: as noted above, pressures at the top of the vapor-dominated zone must exceed the overlying weight of water in order to sustain a flux of steam into the base of the caprock.

Several simulations, including two of those shown in Figure 10, led to vapor-dominated zone pressures in excess of 30.6 bars, the pressure of maximum enthalpy of saturated steam. *James* [1968] and *McNitt* [1977] argued that the pressure at the top of a vapor-dominated zone must be at [James, 1968] or below [McNitt, 1977] 30.6 bars. However, James assumed that large-scale vapor-dominated zones are single-phase steam reservoirs, and McNitt's analysis is more applicable to two-phase systems in which liquid water and steam are flowing cöcurrently. More recent studies agree that near-vaporstatic

vapor-dominated zones are two-phase systems that involve steam-liquid water counterflow, as proposed by *White et al.* [1971]. There appears to be no compelling physical or thermodynamic reason for vapor-dominated zone pressures to be limited to 30.6 bars or less, and an alternate explanation seems to be needed for the coincidence of several systems at about this value.

There is limited field evidence for vapor-dominated zone pressures significantly in excess of 30.6 bars. Dry steam entries from shallow horizons at pressures of 40 bars have been reported at Larderello [*Celati et al.*, 1978], and pressures of around 60 bars have been reported in both shallow and deep horizons at Travale, Tuscany [*Celati et al.*, 1978; *Cappetti et al.*, 1985]. *Hebein* [1983] cited pressures of over 38 bars in the Bottle Rock area of The Geysers, and *Drenick* [1986] presented data from The Geysers that are compatible with vapor-dominated conditions at a depth of more than 2400 m and pressures of over 100 bars. However, some of the excess pressure in these cases may be due to noncondensable gas, and there are not enough pressure measurements in any of these cases to demonstrate a near-vaporstatic pressure profile.

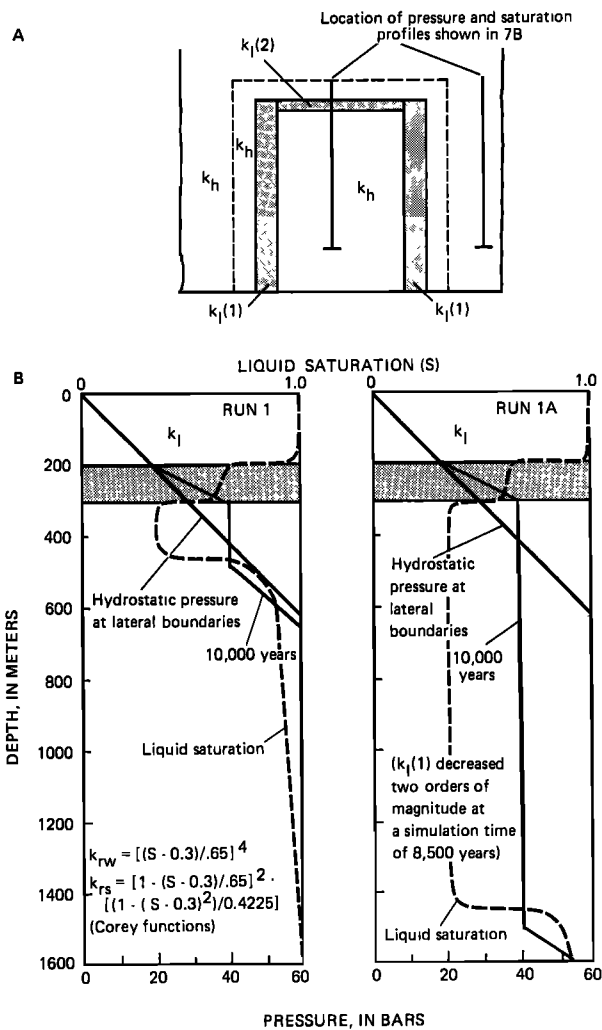


Fig. 7. (a) Diagram defining $k_1(1)$ and $k_1(2)$ and showing the location of the pressure and saturation profiles in Figure 7b. (b) Pressure and saturation profiles at 10,000 years for run 1, showing the effect of decreasing $k_1(1)$ by two orders of magnitude at 8,500 years (run 1A).

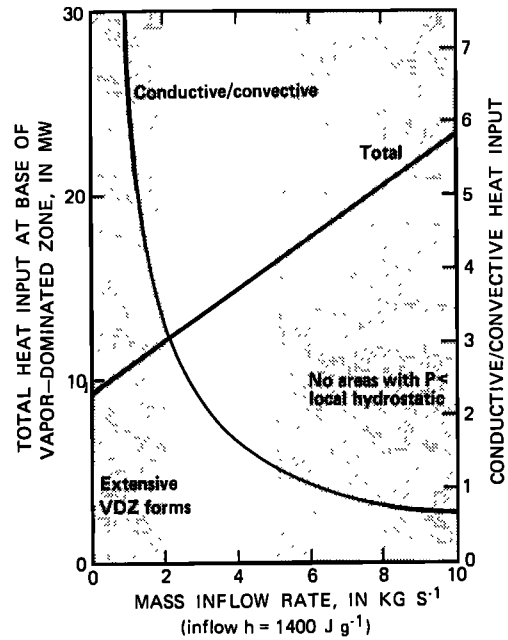


Fig. 8. Total heat input at the lower boundary of the system and ratio of conductive to convective heat input, both as functions of the mass inflow rate M . Conductive heat input exceeds the convective input for $M < 7 \text{ kg s}^{-1}$; with $M_f \leq 2 \text{ kg s}^{-1}$ extensive vapor-dominated zones developed.

The rate of conductive heat loss from deep-high pressure vapor-dominated zones would be relatively small, so such zones might be encountered near the margins of known vapor-dominated systems or on the flanks of intense heat flow anomalies, rather than at the centers of such anomalies. The minimum rate of heat loss from a vapor-dominated zone at various depths can be calculated by assuming that the upper

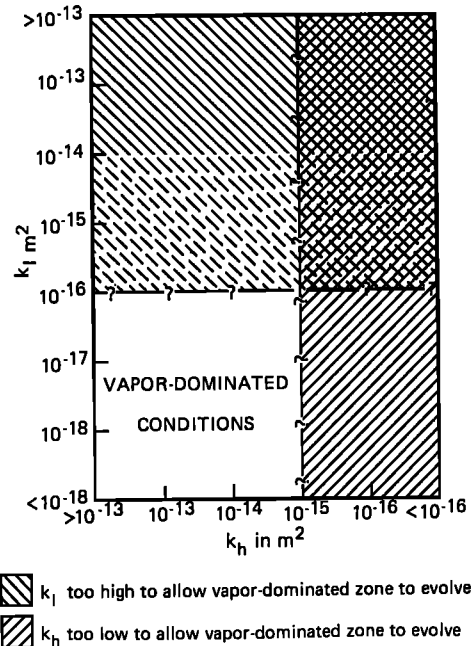


Fig. 9. Permeabilities favorable for the evolution of extensive vapor-dominated zones within the geometric models shown in Figure 4.

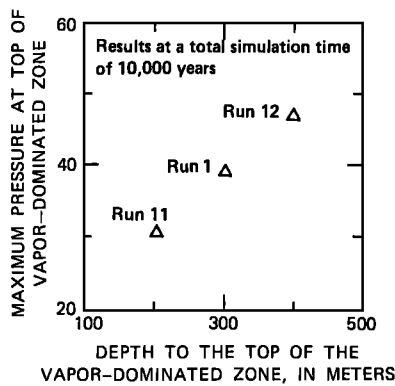


Fig. 10. Relationship between near-steady state vapor-dominated zone pressures and the depth from the upper pressure boundary to the base of the caprock.

pressure boundary is at the land surface; that the heat loss is entirely by conduction to the land surface; and that the temperature at the top of the vapor-dominated zone lies on a hydrostatic boiling-point-with-depth curve (Figure 11). An equivalent rate of heat input at the base of the system would be the minimum required to sustain the vapor-dominated zone.

Factors other than depth can influence pressures in the vapor-dominated zone. For example, a decreasing recharge simulation (Table 1, run 13) that involved a geometric model with a slanted caprock (Figure 4e) but was otherwise similar to run 1 (Figures 5–7) led to higher vapor-dominated zone pressures than any of the other runs (about 60 bars). Because of the geometry of the low-permeability aureole in this model, the conduction of heat from the low-permeability barriers to the boundaries of the system is relatively inefficient, only about one half as efficient as in run 1, for example (Figure 12). So, given the same heat input at the base of the system, higher pressures are needed in the vapor-dominated zone to drive additional steam out and increase the convective heat loss.

Discussion. Our simulations demonstrate that a vapor-dominated zone like that in model I can evolve within low-permeability barriers without changes in boundary conditions or rock properties, given an adequate supply of heat. However, the evolution of the system is more rapid in decreasing recharge cases that involve a relatively high initial fluid throughflow rate that diminishes through time. Another possible mechanism for the evolution of this type of system is a finite period of discharge due to “cracking” of a low-permeability caprock, as demonstrated by Pruess [1985]. Such an event could cause a transition from boiling-point-with-depth conditions to near-vaporstatic conditions by decreasing liquid saturations below the caprock.

For any of these possible mechanisms, factors critical to the evolution of systems like model I are (1) an intense heat source and (2) low-permeability barriers capable of buffering a potential vapor-dominated zone both vertically and laterally. These requirements may account for the apparent scarcity of model I-like systems in nature. The rate of heat input in simulations resulting in formation of persistent vapor-dominated zones (1.5 W m^{-2} in the center of the model) is of the same order as the measured surficial heat flow at The Geysers. Such rates imply relatively shallow depths to magma and large magmatic volumes if persistent through time. The low-permeability aureole must remain intact in order for the vapor-dominated

zone to evolve and persist. Most favorable magmatic heat sources are in tectonically active areas, so that the low-permeability aureole may be breached periodically. Though cracking of a caprock could initiate a vapor-dominated zone, cracking of the lateral barriers would tend to extinguish it. These considerations suggest that few if any large-scale Model I-like systems will reach a true steady state.

Realistic intrusive processes would involve variable rates of heat input. The effects of such variations on the formation and persistence of vapor-dominated zones have not been investigated.

MODELS II AND III

Models II and III (Figures 1b and 1c) both represent systems that have fumaroles and steam-heated discharge at relatively high elevations and high-chloride springs at relatively low elevations. Models II and III differ in terms of the nature and extent of vapor-dominated conditions. These systems are distinct from model I in that the vapor-dominated zones are relatively small and there is a significant throughflow of liquid. The elevation difference between the steam-heated features and the high-chloride springs is essential to drive the systems, whereas in model I fluid circulation is controlled largely by density differences.

In model II, like model I, phase separation occurs at pressures well below local hydrostatic, the pressure gradient within the vapor-dominated zone is near-vaporstatic, and a low-permeability aureole is required to buffer the vapor-dominated zone from surrounding nonthermal groundwater systems (Figure 1b). Although pressures at depth beneath the steam-heated features are generally less than local hydrostatic (Figure 1b), they are everywhere in excess of pressures at similar elevations beneath the high-chloride springs. The maximum thickness of the vapor-dominated zone is roughly constrained by the elevation difference between the steam-heated and high-chloride discharge areas and the pressure gradient required to drive the lateral flow.

In model III, the vapor-dominated conduits are envisioned to be fault or fracture zones of high vertical permeability; there is no overlying low-permeability barrier. Phase separa-

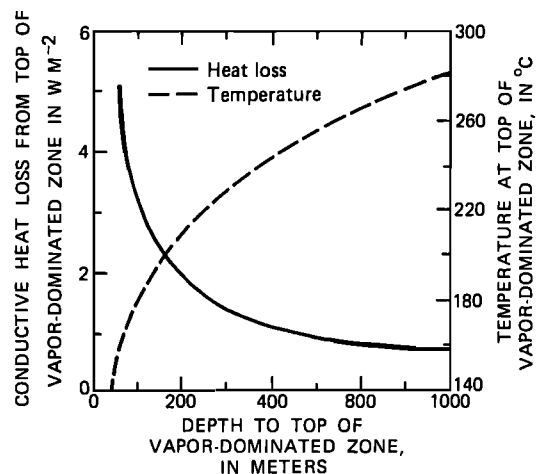


Fig. 11. Minimum heat input rates necessary to sustain a vapor-dominated zone at various depths below an upper pressure boundary, assuming boiling-point-with-depth conditions at the top of the vapor-dominated zone, a temperature of 15°C at the upper boundary, and a thermal conductivity of $1.67 \text{ W m}^{-1} \text{ K}^{-1}$.

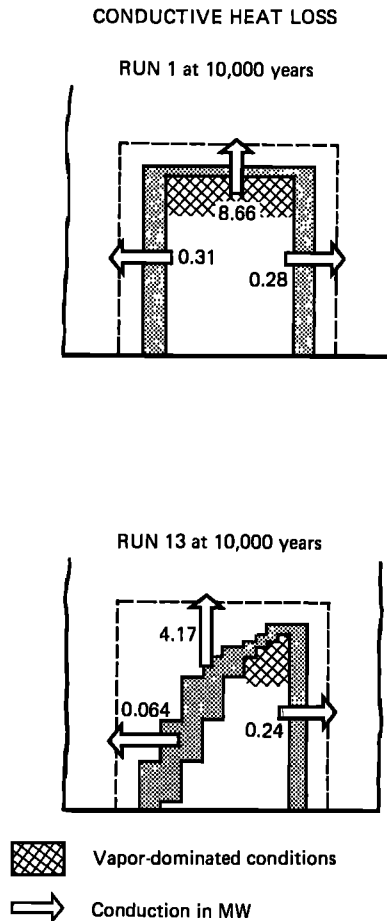


Fig. 12. Rates of conductive heat loss from the vapor-dominated zone, runs 1 and 13. Here the conductive heat loss from the top of the vapor-dominated zone is based on the temperature gradient between the top of the vapor-dominated zone and the upper boundary; in Figure 6 it is based on the temperature gradient between the vapor-dominated zone and the caprock.

tion takes place at pressures close to local hydrostatic pressure, so unless fluid temperatures are unusually high, the zone of phase separation must be within a few hundred meters of the water table. The overall pressure gradient within the vapor-dominated conduits must be near hydrostatic. The pressure gradient tends to be somewhat less than hydrostatic immediately above the area of phase separation and above hydrostatic near the land surface, due to expansion of the rising steam (Figure 1c). Pressures in the vapor-dominated conduits are greater than the pressures in the surrounding liquid-saturated medium.

An essential characteristic of both models II and III is phase separation within a zone of upflow or lateral flow of two-phase fluid. Such phase separation is a result of the density difference between steam and liquid water, which can cause the net forces acting on the two fluids to differ in direction as well as magnitude. In general, if permeable zones exist that allow both vertical and horizontal movement of fluids and provide outlets at different elevations, some degree of phase separation will occur.

Though the surface expressions of models II and III are identical, the differences in terms of the permeability structure and subsurface pressure distribution have both economic and environmental implications. The vertically extensive vapor-

dominated zone under relatively uniform pressure and temperature conditions in model II is an attractive drilling target which is lacking in model III. The response of these two systems to exploitation would differ in the regions where vapor-dominated conditions occur, because of the buffering effect of the thick near-vaporstatic zone beneath the caprock in model II. The steam-heated surface features associated with model II-like systems would be less influenced by pressure changes at depth caused by fluid production.

While model III is of interest as a separate entity, it is important to note that vapor-dominated conduits like those in model III presumably also exist in the condensate zone above the vapor-dominated zone in models I and II. The overall pressure gradient in such conduits must also be near hydrostatic.

Examples

A number of high-temperature systems in mountainous terrain appear to involve large-scale phase separation and thus may be similar to models II and/or III. A partial list of such systems would include Lassen, California [Muffler *et al.*, 1982; Ingebritsen and Sorey, 1985], Baca, New Mexico [Grant, 1979; Grant *et al.*, 1984], La Primavera, Mexico [Mahood *et al.*, 1983], Asal, Djibouti [Correia *et al.*, 1985], Yunatoni [Parmentier and Hayashi, 1981] and Sumikawa (Y. Kubota, written communication, 1986), Japan, and several systems in The Philippines, including Tongonan [Grant, 1979; Grant and Stude, 1981], Palinpinon/Baslay Dauin [Harper and Arevalo, 1983], and Amacan, Mount Apo, and Malindang [Barnett *et al.*, 1985]. There are a number of other possible examples. In some areas a relationship between the steam-heated features and high-chloride springs at lower elevations may be difficult to demonstrate. If the phase separation and lateral flow is relatively deep, the high-chloride waters may be highly diluted and difficult to recognize where they eventually discharge. The phase separation process takes place on a smaller scale in high-temperature systems in gentler terrain, such as Broadlands and Wairakei [Grant, 1979; Allis, 1981] and Rotorua, New Zealand [Ministry of Energy, 1985].

Natural systems can be shown to be similar to either model II or III on the basis of surface observations, though it may not be possible to determine which of the two models is the appropriate one without information on the thickness and pressure distribution within the vapor-dominated zone. Lateral flows of high-chloride fluid and vapor-dominated zones at pressures significantly above atmospheric are essential features of both models. Geochemical techniques can be used to deduce the presence of a lateral flow, if it can be shown that steam-heated features and high-chloride springs are fed by a common source at depth (as at Lassen [Ingebritsen and Sorey, 1985]), and any degree of fumarolic superheat is evidence for vapor-dominated conditions at pressures above atmospheric. Some natural systems may involve an upflow and lateral flow of boiling high-chloride water that feeds more than one vapor-dominated zone, and different models may apply to different regions of the system.

Geometric Models

The geometric models shown in Figure 13 were used to represent models II and III. Both geometric models are two-dimensional vertical cross sections with sloping upper boundaries. The land surface is treated as a constant pressure-enthalpy boundary at a pressure of 1 bar and an enthalpy

equivalent to 15°C, and the lower boundary is a controlled flux boundary. The lateral boundaries are closed to mass and energy. Permeability in the patterned regions (k_l) is low enough that fluid circulation within the models is essentially confined to the vertical conduits along the sides (k_v in model II, and k_v and k_m in model III) and to the lateral conduit (k_h). Fluid circulation is driven by a mass inflow (M) at the lower right, and discharge occurs at the upper right and left sides of the model. A conductive heat flux of 85 mW m⁻² is specified along the base, except in the upflow zone.

The values of permeability and other rock properties shown in Figure 13 were used in all of the simulations and were held constant throughout each simulation. Numerical experiments involved variations in the mass inflow rate M , the enthalpy of the mass inflow, k_h and $k_v(2)$ (model II), and k_m (model III). The width of the vertical conduit on the right-hand side was also varied in model III.

Initial Conditions and Final States

Initial conditions for all of the simulations were a hydrostatic pressure distribution and a low-temperature conductive temperature regime corresponding to a uniform heat flow of 85 mW m⁻². The simulations were continued until pressures and temperatures in the vertical and lateral conduits became relatively stable (temperatures changing less than 1°C/1000 years). In general, the simulations required 10,000–20,000 years to reach this “quasi steady state” condition. Temperatures below the lateral conduit, where heat transport is mostly by conduction, would have taken longer to reach equilibrium.

Individual simulations of models II and III took much less computational time than simulations of model I. The difference in computational time is primarily due to the relatively limited extent of two-phase conditions in models II and III, though there are also fewer finite difference blocks in the grids used to represent these models.

Model II Results

Evolution of systems like model II is likely to begin with a period in which mineralized hot water discharges at the land surface above the main region of upflow. During this period, temperatures in the upflow zone increase to levels such that two-phase conditions can develop when pressures are reduced. At the same time, deposition of silica and carbonate minerals may produce an aureole of relatively low permeability about the upper portion of the upflow zone. Such a feature might also be related to argillization or to preexisting geologic structures and lithologic contrasts; it is necessary to restrict inflow of cooler water during the depressurization and draining of liquid that accompanies the development of a vapor-dominated zone. Fossil sinter deposits in the Devils Kitchen area at Lassen (L. J. P. Muffler, oral communication, 1983) and in the Mud Volcanoes area at Yellowstone [White *et al.*, 1971] provide evidence that high-chloride waters once discharged in certain areas that are now characterized by acid-sulfate discharge.

The vapor-dominated zone in model II can develop within low-permeability barriers by several mechanisms that reverse the direction of liquid flow, allowing water to drain from beneath a low-permeability caprock ($k_v(2)$ in Figure 13) as pressures are lowered to saturation levels and steam replaces liquid. Lateral flow of thermal water toward lower-elevation

outlets is associated with each mechanism. For drainage to occur, the rate of outflow in the lateral conduit must exceed the rate of mass inflow to the system for some period of time.

System evolution: an example. Figures 14 and 15 show results from a simulation in which drainage from beneath a caprock was induced by a decrease in high-enthalpy inflow from 50 to 10 kg s⁻¹. This could result from cooling of a magmatic heat source, which would reduce the fluid density differences that help drive the circulation system; from sealing of flow conduits at depth due to mineral deposition or tectonic activity; or from some combination of these factors.

Values of parameters used in the simulation are listed below or shown in Figure 13.

$$M = 50/10 \text{ kg s}^{-1}$$

$$h = 1125 \text{ J g}^{-1} \text{ (258°C at 100 bars)}$$

$$k_h = 5 \times 10^{-14} \text{ m}^2$$

$$k_v(1) = 1 \times 10^{-13} \text{ m}^2$$

$$k_v(2) = 5 \times 10^{-17} \text{ m}^2$$

$$k_v(3) = 1 \times 10^{-13} \text{ m}^2$$

$$k_{rw} = [(S - 0.3)/0.65]^4$$

$$k_{rs} = [1 - (S - 0.3)/0.65]^2 \times [(1 - (S - 0.3)^2)/0.4225]$$

where k_{rw} and k_{rs} are Corey-type functions for liquid and steam relative permeabilities, S is liquid saturation, and the other parameters are defined in Figure 13. The permeability values for these and other model II simulations were chosen somewhat arbitrarily; our experience with model I and with simulations of the Lassen system [Ingebritsen and Sorey, 1985] suggested that they would lead to the evolution of a vapor-dominated zone.

At early times part of the inflow discharges at higher elevations and heats the upper part of the upflow conduit to more than 200°C and part discharges at lower elevations through the lateral conduit (Figure 14b). The percentage flowing laterally gradually increases as the lateral conduit heats up and fluid viscosity decreases, increasing the hydraulic conductivity of the conduit.

At 1000 years the mass inflow is decreased stepwise to 10 kg s⁻¹, a value less than the flow rate established in the lateral conduit, and liquid begins to drain from beneath the low-permeability caprock. By about 1100 years a vapor-dominated zone is well developed and still growing (Figure 14c), and by about 1900 years it extends down to the top of the lateral conduit. From this point on mass flow rates do not change significantly. At 17,000 years temperatures in the lateral conduit have reached quasi steady state values, but the conduction-dominated temperature regime below the lateral conduit continues to evolve slowly (Figure 14d).

Mass flow vectors at quasi steady state (Figure 14d) show a counterflow of liquid and steam within the vapor-dominated zone, with a net upflow of 0.5 kg s⁻¹. At the base of the caprock layer, some steam condenses and flows downward while the remainder flows into the caprock layer, where it condenses before rising to the land surface. The mass flux of liquid across the land surface represents the discharge of steam and steam condensate at the surface and is equivalent to the net mass upflow of steam through the vapor-dominated zone. As in the simulations of model I, real-world complications involving separate channels for steam and liquid within the

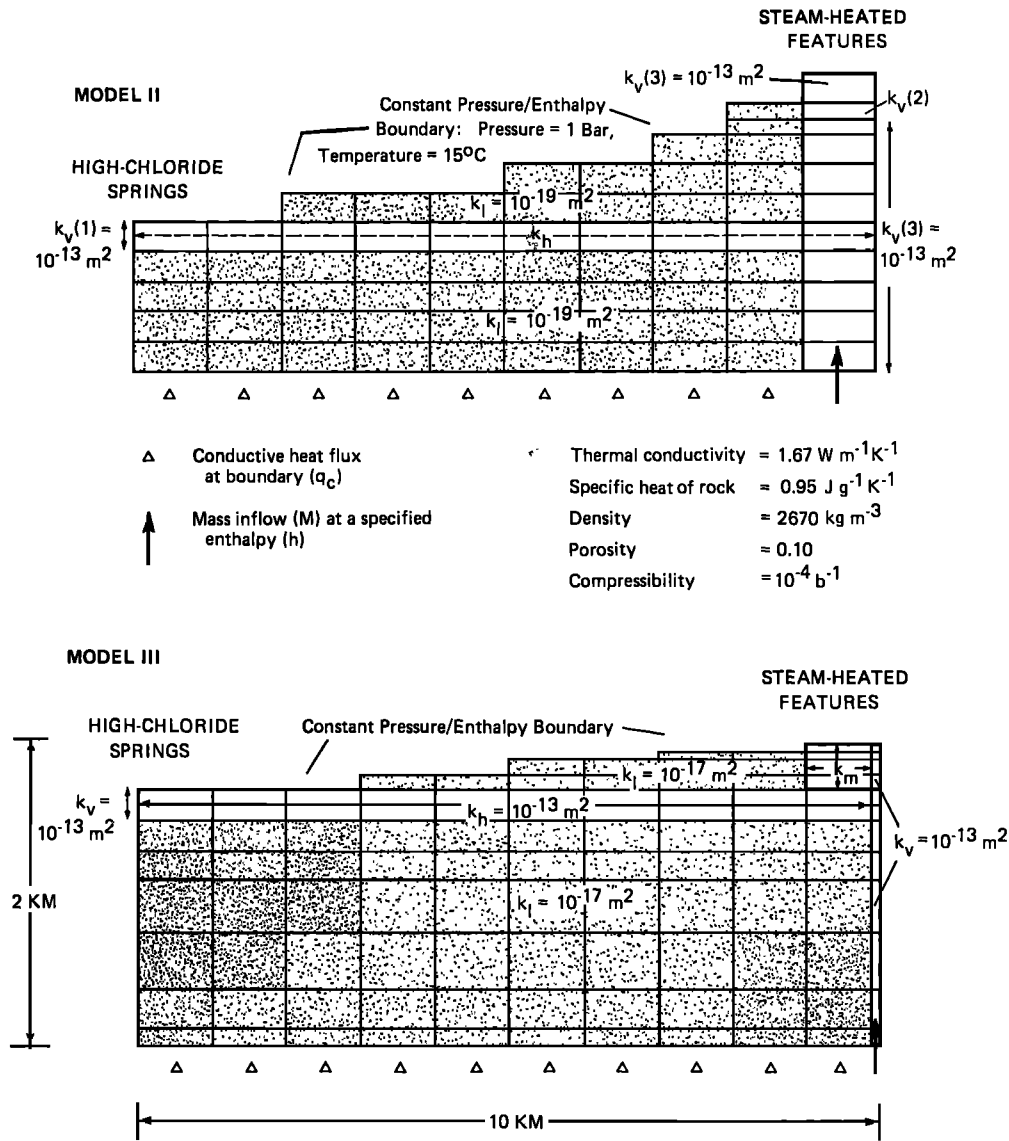


Fig. 13. Geometric models used in numerical simulations of models II and III. The vertical sections are 1 km thick.

condensate zone are neglected. In this simulation the net rate of upflow through the vapor and condensate zones is only about 5% of the lateral outflow rate. Several factors have some influence on the ratio of steam upflow to lateral outflow, including the permeability of the caprock, the inflow enthalpy, and the form of the relative permeability functions, as discussed below. However, in general, the liquid throughflow will not carry enough heat to generate more than 15–20 mass percent vapor.

Simulations in which the drainage process was induced by an increase in permeability along the lateral conduit yielded results similar to those in Figures 14 and 15 except that quasi steady state conditions took longer to develop after drainage was initiated [Ingebritsen and Sorey, 1985]. This was because the lateral conduit was not “preheated” by an initial period with both upflow and lateral outflow. Other possible evolutionary pathways for a model II-like system are discussed by Ingebritsen and Sorey [1985].

In cases that led to the evolution of a vapor-dominated zone, pressures were somewhat greater than hydrostatic above the vapor-dominated zone, and the vertical pressure gradient

was near-vaporstatic within the vapor-dominated zone. As in model I, the excess pressure at the top of the vapor-dominated zone is necessary to allow flow into the low-permeability caprock.

Heat input. The lower boundary condition used for model II is less restrictive than that required for the evolution of a vapor-dominated zone in model I, which involved a high rate of conductive heat input that implied an underlying magmatic heat source. The upflow of thermal fluid that feeds the vapor-dominated zone in Model II need not be strictly vertical or be directly related to a magmatic heat source. It could be fed by a deep circulation system that captures the regional heat flow over a relatively large area. Even if heat is acquired largely from a single magmatic source, the vapor-dominated zone(s) may be offset from the magma body by several kilometers.

Effects of parameter variations. The net rate of upflow of steam within the vapor-dominated zone at quasi steady state depends partly on the caprock permeability ($k_v(2)$). Steam upflow increases as $k_v(2)$ is increased. For example, the net rate of upflow for the simulation shown in Figures 14 and 15 (for which $k_v(2) = 5 \times 10^{-17} \text{ m}^2$) is about 0.5 kg s^{-1} , while a

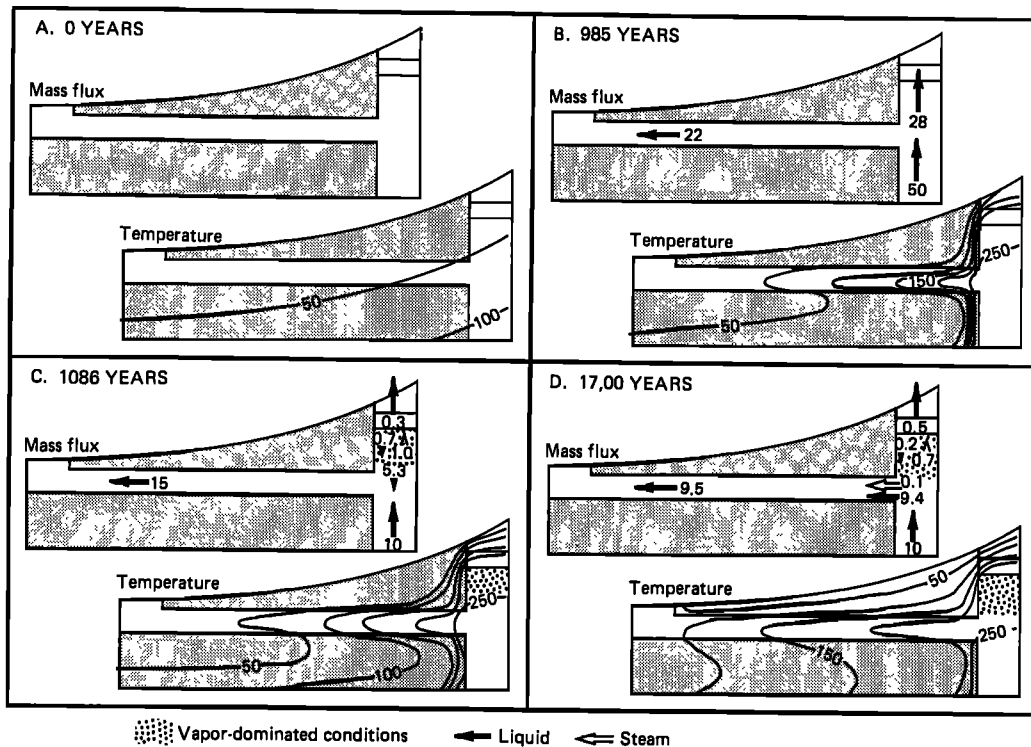


Fig. 14. Mass flow vectors (solid arrows for liquid, open arrows for steam) at selected times during evolution of a system like model II. Mass inflow (M) was reduced from 50 to 10 kg s^{-1} at a simulation time of 1000 years. Dotted pattern represents region of vapor-dominated conditions.

comparable simulation using $k_v(2) = 2.5 \times 10^{-16} \text{ m}^2$ resulted in a net upflow of 1.4 kg s^{-1} .

Liquid saturation in the area of phase separation at the intersection of the lateral and vertical conduits is partly controlled by the inflow enthalpy. Other factors being constant, increasing the inflow enthalpy decreases the liquid saturation in the area of phase separation and increases steam upflow.

For a certain saturation level, various relative permeability functions will also lead to different rates of upflow. In general, however, the form of the relative permeability function is not important in these long-term simulations: steam relative permeabilities approach unity in the vapor-dominated zone, and liquid relative permeability is near unity in the rest of the system, regardless of the functions chosen. The area of phase separation in models II and III is an exception, and will be discussed in more detail under model III results.

The thickness of the vapor-dominated zone in model II is controlled by the depth to the caprock and to the lateral conduit. The vapor-dominated zone begins to develop immediately below the caprock and will exist at quasi steady state only if it extends to the intersection between the lateral and vertical conduits, allowing phase separation in that area. Thus for the geometric model used in the simulations (Figure 13) the vapor-dominated zone is about 700 m thick. Given the same elevation difference between the steam-heated features and the high-chloride springs, the vapor-dominated zone would be thicker if the base of the caprock was shallower or if the lateral conduit dipped down and away from the high-chloride spring area.

In model II (and model III) the extent of liquid-dominated two-phase conditions in the lateral conduit away (down-stream) from the upflow zone is an important factor. If the

fluid in the lateral conduit is two-phase, phase separation can occur wherever the lateral conduit is overlain by zones with high vertical permeability; there can be a number of "satellite" vapor-dominated zones. For the quasi steady state result illustrated in Figure 14d, two-phase flow extends about 4 km

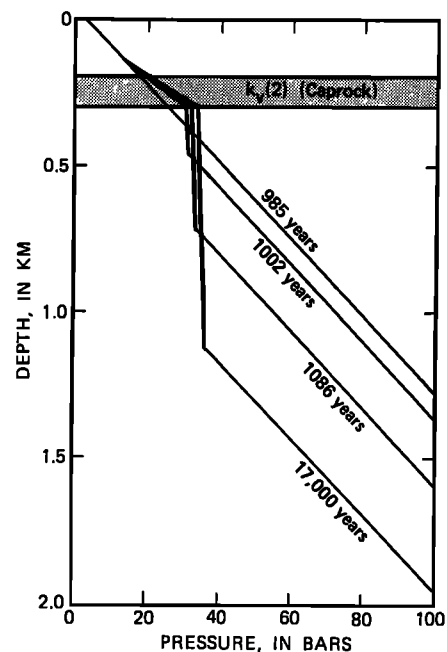


Fig. 15. Pressure profiles in the upflow conduit at selected times during the evolution of a system like model II. Mass inflow was reduced at a simulation time of 1000 years.

downstream from the upflow zone. Factors affecting the extent of liquid-dominated two-phase conditions include the horizontal permeability of the lateral conduit (k_h in Figure 13) and the vertical permeability of the connection between the lateral conduit and the high-chloride springs ($k_v(1)$ and k_v in Figure 13 for models II and III, respectively).

The permeability values required to allow the evolution of a vapor-dominated zone in model II are similar to those required in model I. A rough analogy can be made between k_h (model I) and $k_v(3)$ (model II) and between k_1 (model I) and $k_v(2)$ and k_1 (model II), in terms of the evolution of the vapor-dominated zone. As in model I, a permeability contrast is required at the boundaries of the vapor-dominated zone. For values of caprock permeability ($k_v(2)$) above $2.5 \times 10^{-16} \text{ m}^2$, drainage of liquid across the caprock prevented development of a vapor-dominated zone in model II.

As in model I, pressures within the vapor-dominated zone are directly related to the depth to the caprock, which controls the thickness of the overlying condensate layer. Pressures within the vapor-dominated zone are also affected by any factor that influences the rate of steam upflow, such as the inflow enthalpy (Figure 16).

Model III Results

In model III, as in models I and II, phase separation occurs at pressures well in excess of atmospheric, and within the vapor-dominated zone steam is the more mobile phase. However, the vapor-dominated zone in model III is quite different from those in models I and II in at least two respects: it is nowhere greatly underpressured with respect to local hydrostatic pressure, and the vertical pressure gradient is relatively large. The vertical pressure gradient within the vapor-dominated zone varies significantly with depth, exceeding hydrostatic near the upper boundary. In terms of Figure 2, vapor-dominated zones in models I and II would plot near the result shown for *Ingebritsen and Sorey* [1985]. The vapor-dominated zone in model III would plot outside the lightly patterned region, with $q_s/q_w > 1$ and $k_{rs}/k_{rw} \gg 1$ where the pressure gradient is greater than hydrostatic and with $q_s/q_w < 1$ and $k_{rs}/k_{rw} \gg 1$ where the pressure gradient is subhydrostatic.

The geometric model used to represent model III (Figure 13) allows for a single vapor-dominated conduit ("fracture zone") above the area of phase separation where the lateral and vertical conduits intersect. In a natural system there might be numerous such conduits. Figure 17 shows the upper right hand portion of the geometric model and indicates patterns of fluid circulation when the fracture zone above the area of phase separation is vapor-dominated. Solid arrows represent liquid flow and open arrows represent steam; the double-ended arrows indicate that there may be counterflow in part of the vapor-dominated zone. If a low-permeability caprock was emplaced in the fracture zone, a model II-like vapor-dominated zone might develop in the conduit.

Results of a number of simulations of model III are summarized in Table 2. The mass inflow rate M was 20 kg s^{-1} in all of the simulations; values of other parameters are shown in Figures 13 and 17 or listed in Table 2. Figure 18 shows pressure profiles from two simulations that led to vapor-dominated conditions within the fracture zone. Since phase separation takes place at pressures close to local hydrostatic (Figure 18), the overall pressure gradient within the vapor-dominated conduit must be near-hydrostatic. The pressure

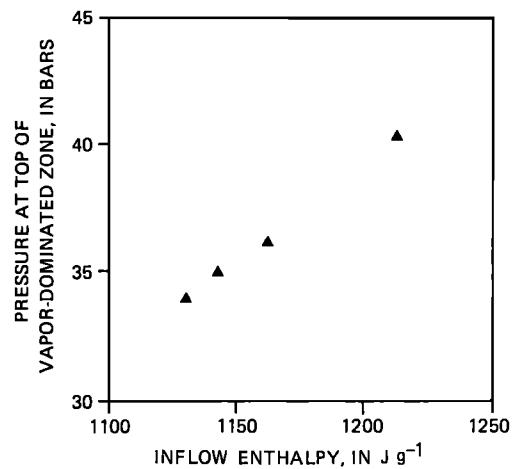


Fig. 16. Effect of inflow enthalpy on vapor-dominated zone pressures in simulations of model II.

gradient tends to be somewhat less than hydrostatic immediately above the area of phase separation and above hydrostatic near the land surface, due to the expansion of the rising steam (see Figure 18).

One of the simulations illustrated in Figure 18 (Figure 18a, run III6) involves Corey relative permeability functions and leads to significant liquid mobility in the fracture zone; the other (Figure 18b, run III8) involves linear relative permeabilities and leads to very low liquid mobility (the various relative permeability functions used are shown in Figure 19). In both cases the permeability of the adjacent "matrix" (k_m in Figures 13 and 17) is 10^{-16} m^2 , and there is some movement of fluid from the fracture zone into the matrix. In both cases $k_{rs}/k_{rw} \gg 1$ near the top of the fracture zone.

System evolution. The vapor-dominated zone in model III can evolve relatively rapidly without changes in rock properties or boundary conditions, given circumstances that allow for a high rate of steam upflow from an area of phase separation. As with model II, evolution of model III-like systems is likely to begin with a period in which hot water discharges at the land surface above the main region of upflow. Over time the upflow zone may be heated to the point that boiling occurs. If two-phase conditions extend to depths such that a conduit with significant lateral permeability is encountered, the phase separation process becomes effective. The steam quality of the two-phase mixture at the land surface will increase as liquid saturation in the area of phase separation decreases. Vapor-dominated conditions may develop quite rapidly in the upper part of the upflow conduit, over periods of tens to hundreds of years within the geometric model used to represent model III (Figure 13).

Drainage of liquid from the evolving vapor-dominated zone was an important component of several of the evolutionary mechanisms suggested for model II. There is no caprock in model III, so such drainage would draw liquid water down from the upper boundary and inhibit rather than favor the development of a vapor-dominated zone. Throughout the evolution of a vapor-dominated zone like that in model III the pressure gradient near the upper boundary must be superhydrostatic.

At early times the lateral conduit is warmed by the outflow, causing fluid viscosity to decrease, so that pressures in the area of phase separation tend to drop. If phase-separation

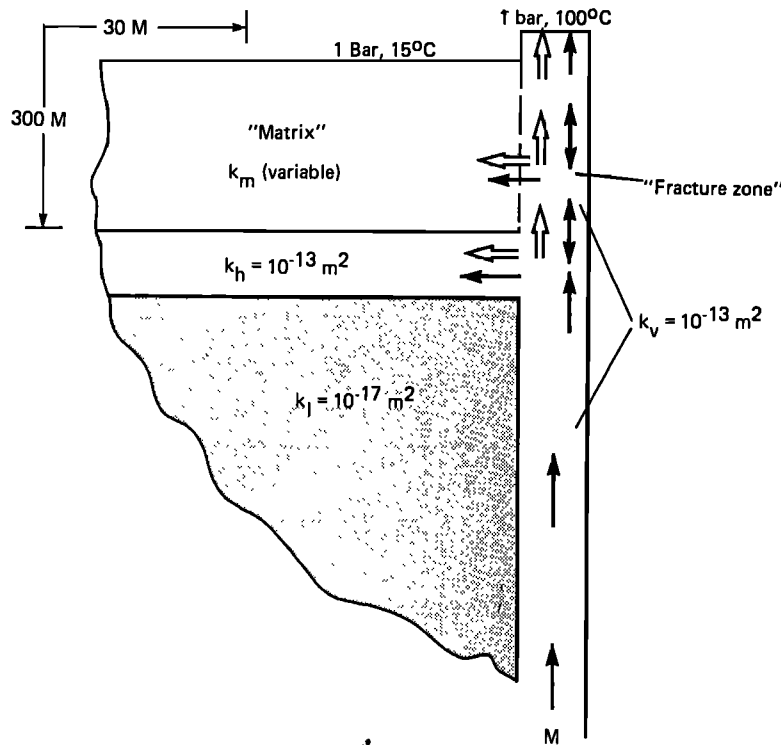


Fig. 17. Part of the geometric model used in simulations of model III, showing patterns of fluid flow when the upper part of the upflow conduit is vapor-dominated. Varying k_m allowed us to examine the degree of lateral isolation necessary for vapor-dominated conditions to develop in the fracture zone. Solid arrows are for liquid, and open arrows are for steam.

pressures become too low and/or the rate of steam upflow is small, there will eventually be drainage from the upper boundary into the fracture zone. If the rate of drainage is high, the steady state result will involve only single-phase liquid downflow through the fracture zone (Table 2, runs III1 and III3). If drainage is relatively sluggish the steady state result may involve liquid-dominated counterflow in the fracture zone (run III4). Vapor-dominated conditions are only stable given near-hydrostatic phase separation pressures and a high rate of steam upflow.

Loss of steam and conductive heat loss into the adjacent "matrix" tend to decrease steam upflow. A decrease in steam upflow causes a decrease in the pressure gradient near the

upper boundary, and may allow downflow of water to extinguish the vapor-dominated zone (Table 2, runs III9 and III-10). For the geometric model used to represent model III, vertical permeability (k_v) in the fracture zone had to be at least 1 to 2 orders of magnitude greater than the horizontal permeability into the matrix to limit steam loss and allow vapor-dominated conditions to develop. The lower value applies to simulations using Corey relative permeability functions, the higher value to simulations using linear and fracture functions, since for intermediate saturation values (such that $k_{rs} \ll 1$ and $k_{rw} \ll 1$) the Corey functions allow much less total flow ($q_s + q_w$) than the others (see Figure 19).

Effects of parameter variations. In general, conditions that

TABLE 2. Summary of Numerical Simulations of Model III

Run	Width of Vertical Conduit, m	Enthalpy of Inflow, $J g^{-1}$	Land Surface Temperature,* $^{\circ}C$	$k_m, \dagger m^2$	Relative Permeability Function	Result
III1	1000	1150	10	1.0×10^{-16}	Corey	single-phase liquid at steady state
III2	1000	1150	100	1.0×10^{-16}	Corey	single-phase liquid at steady state
III3	100	1150	10	1.0×10^{-16}	Corey	single-phase liquid at steady state
III4	100	1150	100	1.0×10^{-16}	Corey	transient vapor-dominated conditions; liquid-dominated counterflow at steady state
III5	10	1150	100	1.0×10^{-16}	Corey	vapor-dominated conditions (?)
III6	10	1300	100	1.0×10^{-16}	Corey	vapor-dominated conditions (?)
III7	10	1300	100	1.0×10^{-16}	fracture	vapor-dominated conditions
III8	10	1300	100	1.0×10^{-16}	linear	vapor-dominated conditions
III9	10	1300	100	1.0×10^{-14}	Corey	vapor-dominated conditions (?)
III10	10	1300	100	1.0×10^{-14}	fracture	oscillatory vapor-dominated conditions

Results are given in terms of conditions in the top part of the vertical conduit on the right-hand side of the geometric model (Figure 13).

*Above upflow zone; the rest of the land surface boundary is at $15^{\circ}C$.

†See Figures 13 or 17.

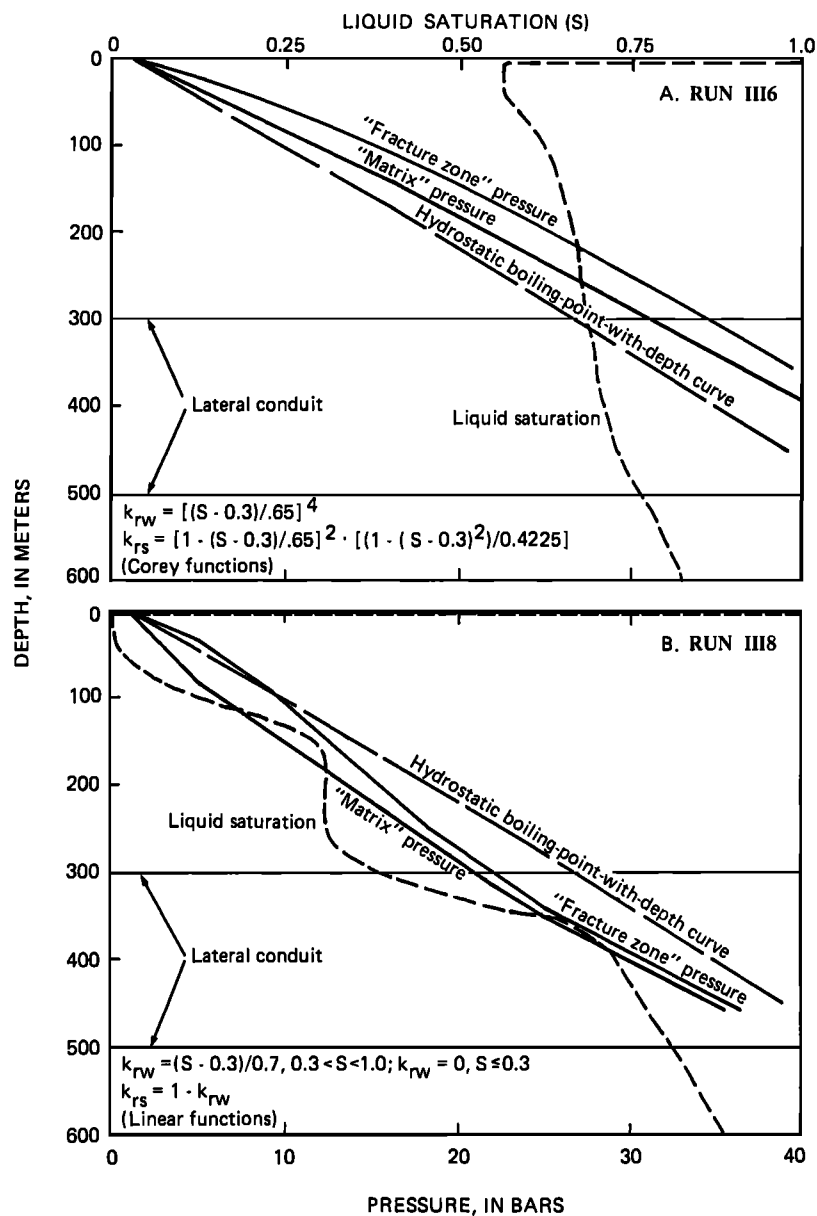


Fig. 18. Pressure and relative permeability profiles at quasi steady state for runs III6 and III8, both of which led to vapor-dominated conditions in the top part of the upflow conduit. Parameters used in these simulations were identical, except that run III6 involves Corey relative permeability functions and run III8 uses linear functions.

increase the steam flux (flow/unit area) from the area of phase separation favor the development of vapor-dominated conditions in the fracture zone. For a given mass inflow M , a higher inflow enthalpy and a narrower fracture zone will increase the steam flux rate. The form of the relative permeability function used is also important, as saturation in the area of phase separation is constrained by the inflow enthalpy and the pressure drop from the base of the model.

Steady state pressures in the area of phase separation in model III are affected by the lateral outflow rate, the permeability of the lateral conduit, the temperature distribution and extent of two-phase conditions within the lateral conduit, and the relative permeability functions chosen. Figure 20 shows quasi steady state fluxes of fluid in and out of the fracture zone for four simulations, three of which (runs III6, III7, and III8) are identical except for the choice of relative

permeability functions. Liquid saturations in the area of phase separation are similar in each case. With the linear and fracture functions there is very little movement of liquid within the fracture zone, whereas with the Corey function $q_w \sim q_s$. Whether the Corey result represents true vapor-dominated conditions is somewhat ambiguous; similar results are queried in Table 2.

Discussion. Since the vertical pressure gradient in the vapor-dominated zone in model III is high, it is not meaningful to choose a single value to represent pressures within the vapor-dominated zone, as we did in analyzing results from models I and II. However, it is instructive to note that in the geometric models representing models II and III phase separation takes place at similar pressures (compare Figures 15 and 18) but at different depths, about 1000 m in model II and 300 m in model III. Because phase separation takes place at pres-

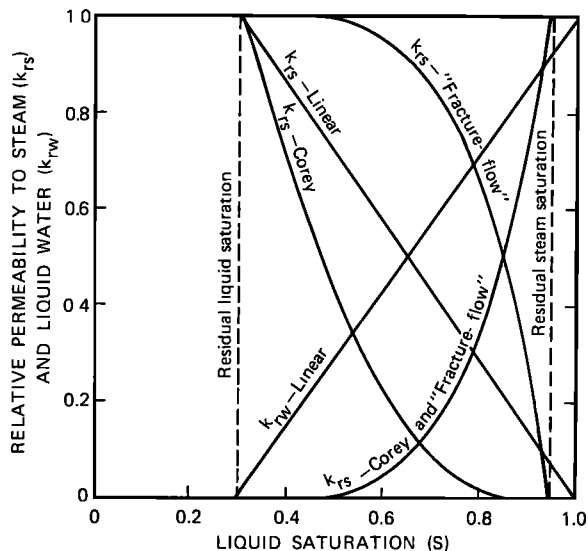


Fig. 19. Relative permeability functions used in simulations of model III. The Corey functions are variations of the empirical functions developed by Corey [1957] for water and air permeability in unsaturated soil. No generally accepted expression has been developed specifically for steam-liquid water relative permeabilities, and the Corey functions are often used in numerical simulations of two-phase hydrothermal systems. However, production data from geothermal reservoirs suggest that Corey-type functions tend to underestimate k_{rs} at most S values and that linear ("x type") or "fracture-flow" [Sorey *et al.*, 1980] functions are more descriptive.

pressures near local hydrostatic in model III, vapor-dominated conditions will not extend to great depths unless fluid temperatures are unusually high.

In model III the net rate of (mass) upflow of steam through the vapor-dominated zone tends to be larger than in model II, given the same mass inflow M . The mass of steam rising from the area of phase separation may be roughly equivalent, but in model II much of the rising steam condenses near the base of the caprock, and the net discharge at the land surface will be smaller. Conceivably, measurements of the rates of lateral outflow and steam discharge could be used to help determine whether model II or model III is the appropriate model for a natural system, but the partitioning would be hard to measure with a high degree of confidence.

In simulations of models I and II real-world complications involving vapor-dominated conduits through the condensate layer were neglected, and the net upflow of steam through the vapor-dominated zone and into the caprock became a liquid discharge at the land surface. In natural systems similar to models I or II the vapor-dominated conduits through the condensate layer may be analogous to the vapor-dominated zone in model III.

SUMMARY

The three model systems discussed in this paper illustrate the range of types of systems in which vapor-dominated conditions are found. Each model involves phase separation at pressures significantly greater than atmospheric and includes a region in which vapor is by far the more mobile phase. Numerical simulation shows that the models are feasible and demonstrates plausible evolutionary pathways for each model. The vapor-dominated zone within each model system is likely

to have evolved from a liquid-dominated state, and for models I and III, this evolution does not require changes in rock properties or boundary conditions.

Systems such as The Geysers, Larderello, Kamojang, and perhaps Matsukawa are generally similar to model I. These systems have low rates of fluid throughflow and extensive vapor-dominated zones with near-vaporstatic pressure gradients. A relatively large number of high temperature systems in mountainous terrain are like models II or III; the surface expression of these models is similar, involving steam-heated features at higher elevations and high-chloride discharge at lower elevations, so that it is difficult to identify the appropriate model for specific systems. Both have relatively high rates of fluid throughflow. The vapor-dominated zone in model II is similar to that in model I, except that it is underlain by a zone of liquid (or liquid-dominated two-phase) throughflow. The vapor-dominated zone in model III is quite different, involving phase separation at pressures near local hydrostatic pressure and an average pressure gradient that is near hydrostatic.

Factors critical to the evolution of a system like model I are

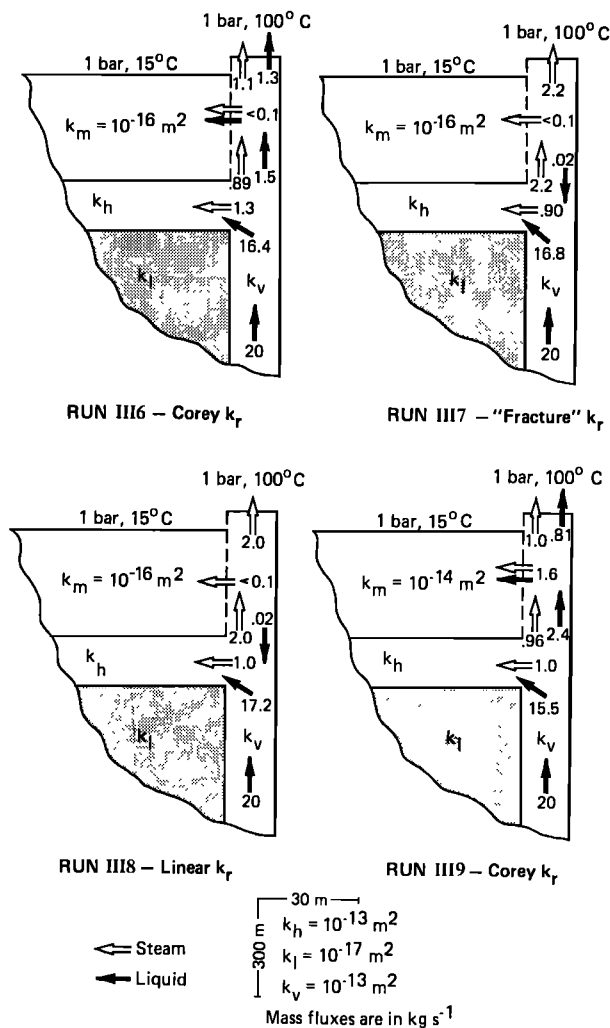


Fig. 20. Mass flow vectors at quasi steady state in four simulations of model III. Solid arrows are for liquid, and open arrows are for steam. Three of the simulations (runs III6-III8) are identical except for the choice of relative permeability functions. Run III9 involves a higher value of k_m (Figures 13 and 17) than run III6, but is otherwise identical.

(1) an intense heat source and (2) low-permeability barriers capable of buffering a potential vapor-dominated zone both vertically and laterally for long periods of time. Permeability within the vapor-dominated zone itself must be relatively high. Since fluid throughflow is limited, the large magnitude of the required heat input implies that the vapor-dominated zone overlies a magmatic heat source. These conditions are quite restrictive, which is consistent with the scarcity of such systems in nature. Under favorable conditions a vapor-dominated zone will begin to develop below a low-permeability caprock and thicken downward. Pressures within the vapor-dominated zone and the thickness of the vapor-dominated zone are shown to be affected by a number of parameters. Within the simple geometric models used, vapor-dominated zone pressure varies regularly with the depth from the upper pressure boundary to the base of the caprock.

Models II and III both require topographic relief and conduits for liquid outflow at relatively low elevations. The lower boundary condition required for the evolution of the vapor-dominated zones in these models is not as restrictive as that in model I; for any model with a dominantly convective heat input the requirement of a very intense local heat source is eliminated.

Several conditions are necessary for the evolution of the vapor-dominated zone in model II, including (1) moderate to great topographic relief; (2) a period of convective heating within an upflow zone followed by (3) some change in hydrologic or geologic conditions that initiates drainage of liquid from portions of the upflow zone; and (4) low-permeability barriers that inhibit the movement of cold water into the evolving vapor-dominated zone. Pressures within the vapor-dominated zone are constrained by the liquid-saturated thickness above the base of the caprock, and are also affected by any parameters that affect the rate of steam upflow from the area of phase separation. The thickness of the vapor-dominated zone in model II is controlled by the permeability structure; that is, by the depths to the caprock and to the lateral conduit.

The vapor-dominated zone in model III can evolve relatively rapidly without changes in rock properties or boundary conditions, given circumstances that allow for a high rate of steam upflow from the area of phase separation. As in model II, evolution of the system is likely to begin with a period in which hot water discharges at the land surface above the main region of upflow. However, there is no period of drainage of liquid; the steam quality of the discharge at the surface simply increases as the liquid saturation in the area of phase separation decreases. In model III the pressure gradient within the vapor-dominated zone near the upper pressure boundary is greater than hydrostatic, so no caprock is needed. The major restriction on the permeability structure is that vertical permeability within the vapor-dominated zone be at least 1 to 2 orders of magnitude greater than the horizontal permeability into the surrounding rocks, a condition that is likely in many fractured rocks. The relatively simple evolution of model III-like systems leads us to speculate that they are relatively common in nature.

Of course, while certain natural systems correlate roughly with one of these models, most are significantly more complex. Many would be better represented as a combination of the models. For example, vapor-dominated conditions like those in model III are probably found locally within the condensate zones of systems similar to models I and II.

APPENDIX

The GEOTHER code solves finite difference approximations to a mass balance equation and an energy balance equation, posed in terms of pressure and enthalpy, respectively. These two variables uniquely define the thermodynamic state of a system. The governing equations are [Faust and Mercer, 1979a]

$$\frac{\delta(n\rho_f l)}{\delta t} - \nabla \cdot \left[\frac{\bar{k}k_{rs}\rho_s}{\mu_s} \cdot (\nabla P - \rho_s g \nabla D) \right] - \nabla \cdot \left[\frac{\bar{k}k_{rw}\rho_w}{\mu_w} (\nabla P - \rho_w g \nabla D) \right] - q_m' = 0 \quad (2)$$

$$\begin{aligned} & \frac{\delta}{\delta t} [n\rho_f l h_f l + (1-n)\rho_r h_r] \\ & - \nabla \cdot \left[\frac{\bar{k}k_{rs}\rho_s h_s}{\mu_s} \cdot (\nabla P - \rho_s g \nabla D) \right] \\ & - \nabla \cdot \left[\frac{\bar{k}k_{rw}\rho_w h_w}{\mu_w} \cdot (\nabla P - \rho_w g \nabla D) \right] \\ & - \nabla \cdot \left[K_m \left(\frac{\delta T}{\delta P} \right)_h \nabla P + K_m \left(\frac{\delta T}{\delta h} \right)_p \nabla h \right] - q_h' = 0 \quad (3) \end{aligned}$$

where

$$\begin{aligned} q_m' &= q_s' + q_w' \\ q_h' &= q_s' h_s' + q_w' h_w' \end{aligned}$$

and the prime denotes a source or sink. The fourth term of (3) reduces to the more familiar form

$$\nabla \cdot K_m \nabla T \quad (4)$$

with ∇T computed indirectly as

$$\left[\left(\frac{\delta T}{\delta P} \right)_h \nabla P + \left(\frac{\delta T}{\delta h} \right)_p \nabla h \right]$$

based on the regression equations describing temperature as a function of pressure and enthalpy. (See the notation list that follows for explanation of the symbols.)

The thermodynamic relationships in the mathematical model are highly nonlinear, as are the relative permeability terms, complicating numerical solution. The nonlinear terms are treated using Newton-Raphson iteration [Faust and Mercer, 1979b, 1982]. This leads to a system of linear equations that must be solved for each iteration. Convergence is checked by calculating an energy and mass balance. Each vertical cross section of the finite difference grid is solved implicitly, so for the two-dimensional problems solved here the solution technique is direct.

NOTATION

- D depth.
- g gravitational acceleration.
- h enthalpy.
- K_m medium thermal conductivity-thermal dispersion coefficient.
- \bar{k} intrinsic permeability tensor.
- k_h zone of relatively high, isotropic permeability, used to describe all of model I except the low-permeability aureole, and the lateral conduit in models II and III.

- k_1 zone of relatively low, isotropic permeability, used to describe the low-permeability aureole in model I and all of models II and III except the lateral and vertical conduits.
- k_m zone of intermediate permeability adjacent to the upper part of the fracture zone in model III.
- k_{rs} relative permeability for steam ($0 \leq k_{rs} \leq 1$).
- k_{rw} relative permeability for water ($0 \leq k_{rw} \leq 1$).
- k_v vertical permeability.
- n porosity.
- P pressure.
- M mass inflow at lower boundary of model.
- q_c conductive heat flux at lower boundary of model.
- q_h flux of energy.
- q_m mass flow rate.
- T temperature.
- t time.
- z elevation.
- ρ density.
- μ dynamic viscosity.
- Subscripts**
- f denotes final.
- $f1$ refers to fluid in place (single- or two-phase mixture).
- i denotes initial.
- m refers to mass.
- r refers to rock.
- s refers to steam.
- w refers to water.

Acknowledgments. Much of this work was done while Ingebritsen was a Ph.D. Candidate at Stanford University, and we would like to thank and acknowledge the other members of the Ph.D. committee: Irwin Remson, Donald E. White, J. D. Bredehoeft, Roland Horne, and R. J. P. Lyon. We would also like to thank Allen Moench and Manuel Nathenson for thorough reviews of the manuscript; Alfred Truesdell for reviewing portions of earlier versions; J. S. Gudmundsson, Karsten Pruess and Terry E. C. Keith for helpful suggestions; and Robert Lowell and an anonymous referee for useful critiques. David Jones drafted most of the figures.

REFERENCES

- Allen, E. T., and A. L. Day, Steam wells and other thermal activity at "The Geysers," California, *Publ. 378, Carnegie Inst. of Washington*, Washington, D. C., 1927.
- Allis, R. G., Changes in heat flow associated with exploitation of Wairakei geothermal field, New Zealand, *N. Z. J. Geol. Geophys.*, 24, 1-19, 1981.
- Barnett, P. R., F. G. Delfin, and O. S. Espanola, Geothermal exploration in the southern Philippines, *Trans. Geotherm. Resour. Council.*, 9(1), 389-394, 1985.
- Cappetti, G., R. Celati, U. Cigni, P. Squarci, G. Stefani, and L. Taffi, Development of deep exploration in the geothermal areas of Tuscany, Italy, *Trans. Geotherm. Resour. Council., Int. Vol.*, 9, 303-309, 1985.
- Celati, R., P. Squarci, G. Stefani, and L. Taffi, Study of water levels at Larderello for reconstruction of reservoir pressure trends, *Geothermics*, 6, 183-198, 1978.
- Corey, A. T., Measurement of water and air permeability in unsaturated soil, *Proc. Soil Sci. Soc.*, 21, 7-10, 1957.
- Correia, H., C. Fouillac, A. Gerard, and J. Varet, The Asal geothermal field (Republic of Djibouti), *Trans. Geotherm. Resour. Council., Int. Vol.*, vol. 513-519, 1985.
- Diner, Y. A., The HY precious metals lode deposit, Mineral County, Nevada, M.S. thesis, Stanford Univ., Stanford, Calif., 1983.
- Drenick, A., Pressure-temperature-spinner surveys in wells at The Geysers, in *Proc. Eleventh Workshop on Geothermal Reservoir Engineering*, pp. 197-206, Stanford University, Stanford, Calif., 1986.
- Faust, C. R., and J. W. Mercer, Geothermal reservoir simulation, 1, Mathematical models for liquid- and vapor-dominated hydrothermal systems, *Water Resour. Res.*, 15, 23-30, 1979a.
- Faust, C. R., and J. W. Mercer, Geothermal reservoir simulation, 2, Numerical solution techniques for liquid- and vapor-dominated hydrothermal systems, *Water Resour. Res.*, 15, 31-46, 1979b.
- Faust, C. R., and J. W. Mercer, Finite-difference model of three-dimensional, single- and two-phase heat transport in a porous medium, Scepter documentation and user's manual, Geotrans, Reston, Va., 1982.
- Geothermal Resources Council, First power plant dedicated at Cove Fort, Utah, *Bull. Geotherm. Resour. Council.*, 14(10), 5-6, 1985.
- Grant, M. A., Interpretation of downhole pressure measurements at Baca, in *Proc. Fifth Workshop on Geothermal Reservoir Engineering*, pp. 261-268, Stanford University, Stanford, Calif., 1979.
- Grant, M. A., and F. E. Studt, A conceptual model of the Tongonan geothermal reservoir, in *Proc. Fourth Conference on Geology, Mineral, and Energy Resources of Southeast Asia*, pp. 823-827, Geological Society of the Philippines, The Bureau of Mines and Geosciences, National Committee on Geologic Sciences, Manila, 1981.
- Grant, M. A., S. K. Garg, and T. D. Riney, Interpretation of downhole data and development of a conceptual model for the Redondo Creek area of the Baca geothermal field, *Water Resour. Res.*, 20, 1401-1416, 1984.
- Gudmundsson, D. S., and S. Thorhallsson, The Svartsengi reservoir in Iceland, *Geothermics*, 15, 3-15, 1986.
- Harper, R. T., and E. M. Arevalo, A geoscientific evaluation of the Baslay-Daun prospect, Negros Oriental, Philippines, *Tech. Bull.*, 1, Philippine Nat. Oil Comp.-Energy Dev. Corp., 1983.
- Hebein, J. J., Exploration, drilling, and development operations in the Bottle Rock area of The Geysers steam field, with new geologic insights and models defining reservoir parameters, in *Proc. Ninth Workshop on Geothermal Reservoir Engineering*, pp. 135-144, Stanford University, Stanford, Calif., 1983.
- Hebein, J. J., Historical hydrothermal evolutionary facets revealed within the exploited Geysers steam field, *Bull. Geotherm. Resour. Council.*, 14(6), 13-16, 1985.
- Ingebritsen, S. E., Evolution of the geothermal system in the Lassen Volcanic National Park area, M.S. thesis, Stanford Univ., Stanford, Calif., 1983.
- Ingebritsen, S. E., Vapor-dominated zones within hydrothermal convection systems: Evolution and natural state, Ph.D. thesis, Stanford Univ., Stanford, Calif., 1986.
- Ingebritsen, S. E., and M. L. Sorey, A quantitative analysis of the Lassen hydrothermal system, north-central California, *Water Resour. Res.*, 21, 853-868, 1985.
- James, Russell, Wairakei, and Larderello, Geothermal power systems compared, *N. Z. J. Sci.*, 11, 706-719, 1968.
- Japan Metals and Chemicals Company, Matsukawa geothermal power development, technical report, Japan Metals and Chemicals Co., Tokyo, 1979.
- Mahood, G. A., A. H. Truesdell, and L. A. Templos, A reconnaissance geochemical study of La Primavera geothermal area, Jalisco, Mexico, *J. Volcanol. Geotherm. Res.*, 16, 247-261, 1983.
- McLaughlin, R. J., Tectonic setting of pre-Tertiary rocks and its relation to geothermal resources in the Geysers-Clear Lake area, *U.S. Geol. Surv. Prof. Pap.*, 1141, 1981.
- McNitt, J. R., Origin of steam in geothermal reservoirs, paper presented at the 52nd Annual Fall Technical Conference and Exhibition, Soc. of Pet. Eng., Dallas, Tex., 1977.
- Mercer, J. W., and C. R. Faust, Geothermal reservoir simulation, 3, Application of liquid- and vapor-dominated hydrothermal modeling techniques to Wairakei, New Zealand, *Water Resour. Res.*, 15, 653-671, 1979.
- Ministry of Energy, The Rotorua Geothermal Field: Technical report of the Geothermal Task Force, 1983-1985, 522 pp., Oil and Gas Div., N.Z. Min. of Energy, Rotorua, 1985.
- Muller, L. J. P., N. L. Nehring, A. H. Truesdell, C. J. Janik, M. A. Clynne, and J. M. Thompson, The Lassen geothermal system, in *Proc. Pacific Geothermal Conference*, pp. 349-356, University of Auckland, Auckland, N.Z., 1982.
- Parmentier, P. P., and M. Hayashi, Geologic model of the "vapor-dominated" reservoir in Yunotani geothermal field, Kyushu, Japan, *Trans. Geotherm. Resour. Council.*, 5, 201-204, 1981.
- Pruess, K., A quantitative model of vapor-dominated geothermal reservoirs as heat pipes in fractured porous rock, *Trans. Geotherm. Resour. Council.*, 9(2), 353-361, 1985.
- Pruess, K., and A. H. Truesdell, A numerical simulation of the natural

- evolution of vapor-dominated hydrothermal systems, in *Proc. Sixth Workshop on Geothermal Reservoir Engineering*, pp. 194–203, Stanford University, Stanford, Calif., 1980.
- Pruess, K., O. Weres, and R. Schroeder, Distributed parameter modeling of a producing vapor-dominated reservoir: Serrazzano, Italy, *Water Resour. Res.*, *15*, 1219–1230, 1983.
- Schubert, G., and J. M. Straus, Steam-water counterflow in porous media, *J. Geophys. Res.*, *84*, 1621–1628, 1979.
- Schubert, G., and J. M. Straus, Gravitational stability of water over steam in vapor-dominated geothermal systems, *J. Geophys. Res.*, *85*, 6505–6512, 1980.
- Sorey, M. L., M. A. Grant, and E. Bradford, Nonlinear effects in two-phase flow to wells in geothermal reservoirs, *Water Resour. Res.*, *16*, 767–777, 1980.
- Sorey, M. L., and S. E. Ingebritsen, A quantitative analysis of the hydrothermal system in Lassen Volcanic National Park and Lassen KGRA, *U.S. Geol. Surv. Water Resour. Invest. Rep.*, *84-4278*, 1984.
- Straus, J. M., and G. Schubert, One-dimensional model of vapor-dominated geothermal systems, *J. Geophys. Res.*, *86*, 9433–9438, 1981.
- Tomasson, J., and H. Kristmannsdottir, High temperature alteration minerals and thermal brines, Reykjanes, Iceland, *Contrib. Miner. Petrol.*, *36*, 123–134, 1972.
- Tomasson, J., and O. B. Smarason, Developments in geothermal energy, Hydrogeology in the service of man, in *Memoires of the 18th Congress of the International Association of Hydrogeologists*, pp. 189–211, Cambridge, England, 1985.
- White, D. E., L. J. P. Muffler, and A. H. Truesdell, Vapor-dominated hydrothermal systems compared with hot-water systems, *Econ. Geol.*, *66*, 75–97, 1971.
-
- S. E. Ingebritsen and M. L. Sorey, U.S. Geological Survey, 345 Middlefield Road, Menlo Park, CA 94025.

(Received August 10, 1987;
revised May 16, 1988;
accepted July 15, 1988.)